The clinical implication and molecular mechanism of preferential IL-4 production by modified glycolipid-stimulated NKT cells

Shinji Oki, Asako Chiba, Takashi Yamamura, and Sachiko Miyake

Department of Immunology, National Institute of Neuroscience, National Center for Neuroscience and Psychiatry, Tokyo, Japan.

OCH, a sphingosine-truncated analog of α-galactosylceramide (αGC), is a potential therapeutic reagent for a variety of Th1-mediated autoimmune diseases through its selective induction of Th2 cytokines from natural killer T (NKT) cells. We demonstrate here that the NKT cell production of IFN-γ is more susceptible to the sphingosine length of glycolipid ligand than that of IL-4 and that the length of the sphingosine chain determines the duration of NKT cell stimulation by CD1d-associated glycolipids. Furthermore, IFN-γ production by NKT cells requires longer T cell receptor stimulation than is required for IL-4 production by NKT cells stimulated either with immobilized mAb to CD3 or with immobilized "αGC-loaded" CD1d molecules. Interestingly, transcription of *IFN-γ* but not that of *IL-4* was sensitive to cycloheximide treatment, indicating the intrinsic involvement of de novo protein synthesis for IFN-γ production by NKT cells. Finally, we determined *c-Rel* was preferentially transcribed in αGC-stimulated but not in OCH-stimulated NKT cells and was essential for IFN-γ production by activated NKT cells. Given the dominant immune regulation by the remarkable cytokine production of ligand-stimulated NKT cells in vivo, in comparison with that of (antigen-specific) T cells or NK cells, the current study confirms OCH as a likely therapeutic reagent for use against Th1-mediated autoimmune diseases and provides a novel clue for the design of drugs targeting NKT cells.

Introduction

Natural killer T (NKT) cells are a unique subset of T lymphocytes that coexpress the α/β T cell receptor (TCR) along with markers of the NK lineage such as NK1.1, CD122, and various Ly49 molecules. Most NKT cells express an invariant TCRα chain composed of Vα14-Jα281 segments in mice and Vα24-JαQ segments in humans associated with a restricted set of Vβ genes (1, 2). Unlike conventional T cells, which recognize peptides presented by MHC molecules, NKT cells recognize glycolipid antigens such as α-galactosylceramide (αGC) in the context of a nonpolymorphic MHC class I-like molecule, CD1d (3–5). After being stimulated by a ligand, NKT cells rapidly affect the functions of neighboring cell populations such as T cells, NK cells, B cells, and dendritic cells (6, 7). The various functions of NKT cells are mediated mainly by a rapid release of large amounts of cytokines, including IL-4 and IFN-γ. Whereas IFN-γ provides help for the Th1 responses required for defending against various pathogens and tumors, IL-4 controls the initiation of Th2 responses and has been shown to inhibit Th1-mediated autoimmune responses involved in experimental autoimmune encephalomyelitis (EAE), collagen-induced arthritis (CIA), and type 1 diabetes in NOD mice.

Given the exceptional ability of NKT cells to secrete regulatory cytokines in comparison with that of T cells or NK cells after primary stimulation, we have explored the possibility that ligand stimulation of NKT cells may lead to the suppression of Th1-mediated autoimmune diseases. We have previously demonstrated that OCH, a sphingosine-truncated analog of αGC, preferentially induces Th2 cytokines from NKT cells and that administration of OCH suppresses EAE and CIA by inducing a Th2 bias in autoantigen-reactive T cells (8, 9). However, the molecular mechanism accounting for the unique property of OCH to selectively induce IL-4 has not been clarified yet.

In this study, we used various stimuli, including the prototypic ligand αGC and its derivatives such as OCH, to investigate the molecular basis of the differential production of IL-4 and IFN-γ by NKT cells. We found that OCH, due to its truncated lipid chain, was less stable in binding the CD1d molecule than was αGC and exerted short-lived stimulation on NKT cells. IFN-γ production by NKT cells required longer TCR stimulation than was required for IL-4 production and de novo protein synthesis. *c-Rel* was preferentially transcribed in αGC-stimulated, but not in OCH-stimulated NKT cells and was shown to regulate IFN-γ production by NKT cells. Taken together, these results indicate that sustained TCR stimulation and concomitant c-Rel expression by αGC leads to the production of IFN-γ, whereas short-term activation and marginal *c-Rel* transcription by OCH results in preferential production of IL-4 by NKT cells.

Methods

Mice. C57BL/6 (B6) mice were purchased from CLEA Laboratory Animal Corp. (Tokyo, Japan). MHC class II–deficient I-$A^b\beta^{-/-}$ mice were purchased from Taconic (Germantown, New York, USA). All animals were kept under specific pathogen-free conditions and were used at 7–10 weeks of age. Animal care and use were in accordance with institutional guidelines.

Cell lines, antibodies, plasmids, and reagents. The NKT cell hybridoma (N38.2C12) (10) was a generous gift from K. Hayakawa (Fox Chase Cancer Center, Philadelphia, Pennsylvania, USA) and NS0-derived

Nonstandard abbreviations used: altered glycolipid ligand (AGL); altered peptide ligand (APL); CD28 responsive element (CD28RE); collagen-induced arthritis (CIA); c-Rel lacking C-terminal transactivation domain (c-RelΔTA); cycloheximide (CHX); cyclosporin A (CsA); experimental autoimmune encephalomyelitis (EAE); α-galactosylceramide (αGC); natural killer T (NKT); nuclear factor of activated T cell (NF-AT); phycoerythrin (PE); T cell receptor (TCR).

Conflict of interest: The authors have declared that no conflict of interest exists.

Citation for this article: *J. Clin. Invest.* **113**:1631–1640 (2004). doi:10.1172/JCI200420862.

plasmacytoma cell lines expressing the Kb tail mutant of CD1d (11) were kindly provided by S. Joyce (Vanderbilt University, Nashville, Tennessee, USA). Cells were maintained in RPMI 1640 medium supplemented with 10% FCS, 2 mM L-glutamine, 100 U/ml penicillin/streptomycin, 2 mM sodium pyruvate, and 50 μM β-mercaptoethanol (complete medium). Phycoerythrin (PE)-labeled mAb to NK1.1 (PK136), peridinine chlorophyll protein/cyanine 5.5 -labeled mAb to CD3 (2C11), and recombinant soluble dimeric human CD1d:Ig fusion protein (DimerX I) were from BD PharMingen (San Diego, California, USA). For some experiments mAb's to NK1.1 (PK136) and CD3 (2C11) were conjugated with FITC. Polyclonal antibody to asialo GM_1 was purchased from WAKO Chemicals (Osaka, Japan). The pRc/CMV-c-Rel expression plasmid (12) was a generous gift from Grundström (Umeå University, Umeå, Sweden). The open reading frame of c-Rel cDNA was amplified by PCR and cloned into the retroviral pMIG(W) vector. The forward primer containing the *Xho*I recognition site was 5′-GACTCTCGAGATGGCCTCGAGTGGATATAA-3′ and the reverse primers used for wild-type c-Rel or the dominant negative mutant c-RelΔTA containing *Eco*RI recognition sites were 5′-GACTGAATTCTTATATTTTAAAAAAACCATATGTGAAGG-3′ and 5′-GACTGAATTCTTAACTCGAGATGGACCCGCATG-3′, respectively. The retroviral vector (pMIG) and packaging vector (pCL-Eco) were kindly provided by L. Van Parijs (Massachusetts Institute of Technology, Cambridge, Massachusetts, USA). Cyclosporin A (CsA) and cycloheximide (CHX) were from Sigma-Aldrich (St. Louis, Missouri, USA). All glycolipids were prepared as described in the Supplemental Methods (supplemental material available at http://www.jci.org/cgi/content/full/113/11/1631/DC1). The glycolipids were solubilized in DMSO (100 μg/ml) and were stored at -20°C until use.

Kinetic analysis of glycolipid stability on CD1d molecules. The kinetic analysis of glycolipid stability on CD1d molecules was performed as described previously with slight modifications (13). In brief, the NKT hybridoma was preincubated with 4 μM Fura red and 2 μM Fluo-4 (Molecular Probes, Eugene, Oregon, USA) at room temperature for 45 minutes, washed with RPMI 1640 medium containing 2% FCS (assay media), and resuspended in assay media. For determination of the optimal time for glycolipid loading onto $CD1d^+$ APCs, kinetic analysis was conducted using either αGC or OCH. According to the data obtained in Figure 2C, $CD1d^+$ APCs were pulsed with glycolipids (100 ng/ml) for 30 minutes. Then, cells were washed and resuspended in assay media. Glycolipid-pulsed APCs were harvested every 15 minutes after resuspension, mixed with NKT cells, and subjected to centrifugation in a table-top centrifuge (2,000 *g*) for 60 seconds. Cells were then resuspended briefly and analyzed for calcium influx into NKT hybridoma cells by flow cytometry (EPICS XL; Beckman Coulter, Tokyo, Japan). Activation was expressed as the percentage of Fura-red– and Fluo-4–stained cells in a high-FL1, low-FL4 gate.

In vivo glycolipid treatment and microarray analysis. Mice were injected intraperitoneally with 0.2 ml PBS containing 0.1 mg anti-asialo GM_1 Ab. Forty hours after injection, mice were injected intraperitoneally with αGC, OCH (100 μg/kg), or control vehicle in 0.2 ml PBS. After the indicated time point, liver mononuclear cells or spleen cells were harvested and NKT cells were purified with the AUTOMACS cell purification system using FITC-conjugated mAb to NK1.1 (PK136) and anti-FITC microbeads (Miltenyi Biotech GmbH, Bergisch Gladbach, Germany). The purity of NKT cells in the untreated samples and in the samples treated for 1.5 hours was more than 90%. The purity of the liver-derived samples and spleen-derived samples treated for 12 hours was more than 80% and 74%, respectively. Total RNA isolation with the RNeasy Mini Kit (Qiagen, Chatsworth, California, USA) and whole-microarray procedures using U74Av2 arrays (GeneChip System; Affymetrix, Santa Clara, California, USA) were done according to the manufacturers' instructions. From data image files, gene transcript levels were determined using algorithms in the Gene Chip Analysis Suit software (Affymetrix). Each probe was assigned a "call" of present (expressed) or absent (not expressed) using the Affymetrix decision matrix. Genes were considered to be differentially expressed when (a) expression changed at least threefold in the case of liver NKT-derived samples or twofold in the case of spleen NKT-derived samples compared with the expression in the negative control and (b) increased gene expression included at least one "present call."

In vitro stimulation. Liver mononuclear cells were isolated from B6 mice by Percoll density gradient centrifugation and were stained with PE-NK1.1 and FITC-CD3 mAb's. The $CD3^+NK1.1^+$ cells and $CD3^-NK1.1^+$ cells were sorted with an EPICS ALTRA Cell Sorting System (Beckman Coulter). The purity of the sorted cells was more than 95%. Sorted cells were suspended in RPMI 1640 medium supplemented with 50 μM 2-mercaptoethanol, 2 mM L-glutamine, 100 U/ml penicillin and streptomycin, and 10% FCS and were stimulated with immobilized mAb to CD3. Incorporation of [^{3}H]thymidine (1 μCi/well) for the final 16 hours of the culture was analyzed with a β-1205 counter (Pharmacia, Uppsala, Sweden). We measured the content of cytokines in the culture supernatants by ELISA. For quantitative PCR analysis, we harvested the cells after stimulation with glycolipid to prepare total RNA. Glycolipid stimulation of spleen cells in vitro was done similarly except that 1% syngeneic mouse serum was used instead of FCS. In some experiments, plates were coated with DimerX I (1 μg in 50 μl PBS per well) for 16 hours. After plates were washed extensively with PBS, glycolipids (100–200 ng in 50 μl PBS per well) were added, followed by incubation for another 24 hours. Then, NKT cells were added and cytokine production was analyzed after 72 hours of incubation.

Real-time PCR to monitor gene expression. Real-time PCR was conducted using a Light Cycler-FastStart DNA Master SYBR Green I kit (Roche Diagnostics GmbH, Mannheim, Germany) according to the manufacturer's specifications using 4 mM $MgCl_2$ and 1 pM primers. Values for each gene were normalized to those of a housekeeping gene (*GAPDH*) before the "fold change" was calculated (using crossing point values) to adjust for variations between different samples. Primers used for the analysis of gene expression are described in Supplemental Methods.

ELISA. For evaluation of cytokine production by NKT cells, sorted liver $CD3^-NK1.1^+$ NKT cells were stimulated with immobilized mAb to CD3 in complete medium. The level of cytokine production in cell culture supernatants or in serum was determined by standard sandwich ELISA using purified and biotinylated mAb sets and standards from BD PharMingen. After the addition of a substrate, the reaction was evaluated using a Microplate reader (BioRad).

Retroviral infection of NKT cells. The 293T cells were maintained in DMEM supplemented with 10% FCS, 2 mM L-glutamine, 100 U/ml penicillin/streptomycin, 2 mM sodium pyruvate, and 50 μM β-mercaptoethanol. Liver mononuclear cells were purified and cultured in complete medium supplemented with IL-2 (200 U/ml) for 24–48 hours. Cells were infected with retrovirus prepared by cotransfection of pMIG retroviral vector and pCL-Eco packaging vector into 293T cells. Cells were cultured in complete medium containing IL-2 and IL-15 (50 ng/ml) continuously for 3 days, and

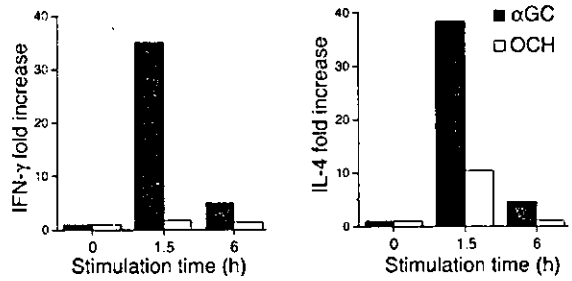

Figure 1
Transcriptional upregulation of cytokine genes by NKT cells stimulated with glycolipids in vivo. B6 mice were injected intraperitoneally with αGC or OCH (100 μg/kg), and liver NKT cells were isolated at the indicated time point. Total RNA was extracted and analyzed for cytokine mRNA by quantitative RT-PCR as described in Methods. Data are presented as "fold induction" of cytokine mRNA after glycolipid treatment. The amount of mRNA in NKT cells derived from untreated animals was defined as 1.

GFP-positive NKT cells were sorted and stimulated with immobilized mAb to CD3 for 48 hours. Culture supernatants were subjected to evaluation of cytokine production by ELISA.

Results

Preferential IL-4 production by OCH-stimulated NKT cells. The suppression of EAE by OCH was found to be associated with a Th2 bias of autoimmune T cells mediated by IL-4 produced by NKT cells (9). To confirm the primary involvement of NKT cells in the Th2 bias seen in the OCH treatment, we purified CD3$^+$NK1.1$^+$ NKT cells from B6 mice treated in vivo with αGC or OCH and measured the transcription of cytokine genes by quantitative RT-PCR. As shown in Figure 1, treatment with αGC greatly increased the expression of both IFN-γ and IL-4 at 1.5 hours after injection, whereas OCH induced a selective increase in IL-4 expression. When the IL-4/IFN-γ ratio was used for evaluating the Th1/Th2 balance, the NKT cells, isolated at 1.5 hours after injection of OCH were distinctly biased toward Th2 (Table 1). These results indicate that OCH is a selective inducer of rapid IL-4 production by NKT cells when administered in vivo.

Lipid chain length and cytokine production. Comparison of the structural difference between OCH and αGC (Figure 2A) raised the possibility that the lipid chain length of the glycolipid ligand may influence the cytokine profile of glycolipid-treated NKT cells. We compared αGC and OCH as well as newly synthesized analogs F-2/S-3 and F-2/S-7, which bear lipids of intermediate length (Figure 2A), for their ability to induce cytokine production by splenocytes. There was good correlation between the lipid tail length of each glycolipid and its ability to induce IFN-γ from the splenocytes, and a larger amount of IFN-γ was released into the supernatants after stimulation with the glycolipids with the longer sphingosine chain (Figure 2B, right). Regarding the ability to stimulate IL-4 production, the differences among OCH, F-2/S-3 and F-2/S-7 were less clear, as shown by IFN-γ induction. Similar results were obtained with liver mononuclear cells as responder cells (see Supplemental Figure 1). These results indicate that cytokine production by NKT cells, in particular IFN-γ production, is greatly influenced by lipid chain truncation of the glycolipid.

Differential half-life of NKT cell stimulation by CD1d-associated glycolipids. It is believed that the two lipid tails of the glycolipids (sphingosine base and fatty acyl chain) would be accommodated by the highly hydrophobic binding grooves of CD1d. To verify the hypothesis that the functional properties of each glycolipid may be determined by the stability of its binding to CD1d molecules, we evaluated the half-life of these glycolipids on CD1d molecules by estimating calcium influx into NKT hybridoma cells as described previously (13). To exclude the possible involvement of endosomal/lysosomal sorting in this assay, we used APCs expressing a CD1d mutant (Kb tail) that lacks the endosomal/lysosomal targeting signal (11). The cells express both β_2m and sCD1d1 fused to the transmembrane and cytosolic tail sequence of H-2K^b at the carboxyl terminus and could bind to glycolipids such as αGC or OCH without their internalization and following endosomal/lysosomal sorting. Based on the kinetic analysis data for glycolipid loading efficiency shown in Figure 2C, we pulsed CD1d$^+$ APCs with glycolipids for 30 minutes.

Figure 2D shows that OCH was rapidly released from the CD1d molecule. A 30% reduction in calcium influx was observed after 15 minutes of incubation and only 25% of the initial amount of glycolipid remained after 60 minutes of incubation. In contrast, αGC was not released from CD1d molecule in the first 15 minutes and more than 50% of the initial amount of glycolipid remained after 60 minutes of incubation. F-2/S-3 and F-2/S-7 showed intermediate levels of release from CD1d molecule. These results support the idea that a glycolipid with a shorter sphingosine chain has a shorter half-life for NKT cell stimulation because of less-stable association with the CD1d molecule.

Kinetic analysis of cytokine production by activated NKT cells. Previous in vivo studies demonstrated that injection of αGC into B6 mice can induce a rapid and transient elevation of the serum IL-4 level and a delayed and persistent rise in IFN-γ (9, 14), suggesting that there is an intrinsic difference in kinetics for the production of IL-4 and IFN-γ by NKT cells. To address this issue further, we sorted CD3$^+$NK1.1$^+$ NKT cells, and conventional CD3$^+$NK1.1$^-$ T cells as a control, from liver lymphocytes and stimulated the sorted cells with immobilized mAb to CD3 for various periods of time. The cells were then incubated at rest without further stimulation and culture supernatants were harvested at 72 hours after initiation of the TCR stimulation. We found that TCR stimulation of NKT cells for as little as 2 hours could induce detectable IL-4 in the supernatant (Figure 3A, center). The amount of IL-4 in the supernatant rapidly increased in proportion to the duration of TCR stimulation (Figure 3A, center). In contrast, production of IFN-γ by NKT cells required at least 3 hours of TCR stimulation and gradually increased corresponding to the duration of TCR stimulation (Figure 3A, right). Conventional T cells required longer TCR stimulation for efficient cytokine production. We repeatedly confirmed that IFN-γ production by NKT cells required initial stimulation that was 1–2 hours longer and showed a slower accumulation than that of IL-4 production in this experimen-

Table 1
Transcriptional upregulation of cytokine genes by NKT cells stimulated with glycolipids in vivo

Stimulus	Time	*IFN-γ*	*IL-4*	Ratio (*IL-4*/*IFN-γ*)
αGC	1.5 h	35.0	38.3	1.09
	6 h	5.0	4.6	0.92
OCH	1.5 h	1.8	10.3	5.58
	6 h	1.5	1.1	0.72

The relative amounts of transcripts of *IFN-γ* and *IL-4* obtained from the experiment shown in Figure 1 are presented as "fold induction" relative to that of NKT cell–derived samples from untreated animals.

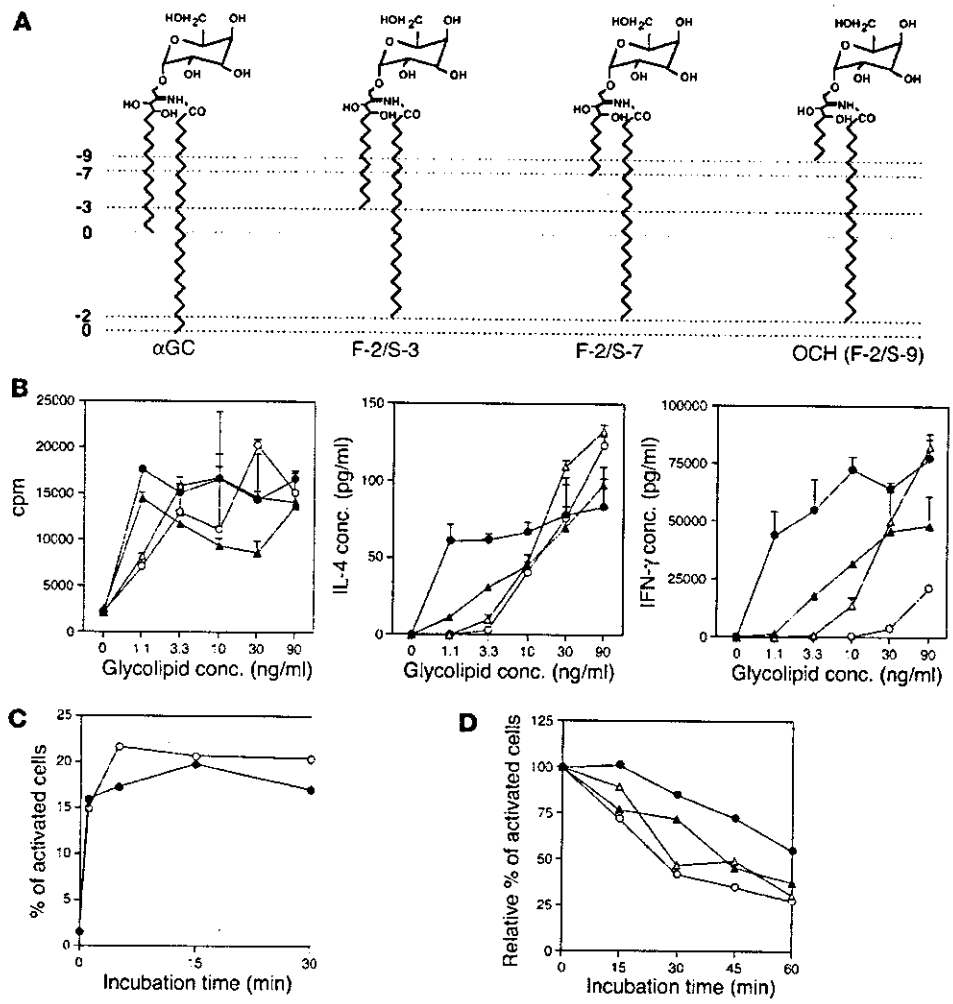

Figure 2

Differential properties of structurally distinct glycolipid derivatives. (**A**) Structures of αGC, OCH, and two other glycolipid ligands for NKT cells. F-2/S-3 has a truncation of two hydrocarbons in the fatty acyl chain (F) and of three hydrocarbons in the sphingosine chain (S) in comparison with αGC. OCH can be called F-2/S-9 accordingly. The numbers of truncated hydrocarbons in either lipid chain are shown along the left margin as negative integers. (**B**) Effect of αGC, OCH, and other glycolipids on proliferation and cytokine production of splenocytes. Splenocytes were stimulated with various concentrations (conc.) of αGC (filled circles), OCH (open circles), F-2/S-3 (filled triangles), or F-2/S-7 (open triangles) for 72 hours. Incorporation of [^{3}H]thymidine (1 μCi/well) during the final 16 hours of the culture was assessed (left), and IL-4 (center) or IFN-γ (right) in the supernatants was measured by ELISA. (**C**) Kinetic analysis of the loading of αGC (filled circles) or OCH (open circles) onto CD1d$^+$ APCs. See Methods for details. One experiment representative of two independent experiments with similar results is shown. (**D**) Calcium influx into NKT hybridoma cells after coculture with CD1d$^+$ APCs pulsed with αGC, OCH, F-2/S-3, or F-2/S-7. Data are presented as the activity remaining when the respective activity of glycolipid-loaded APCs for activation of the NKT cell hybridoma at time 0 was defined as 100%. Data are representative of three experiments with similar results.

tal setting. A similar kinetic difference was also observed when we used spleen-derived NKT cells (data not shown). These results indicate that NKT cells could produce IL-4 after a shorter period of TCR stimulation than is required for IFN-γ production.

To exclude the possibility that a qualitatively different CD1d complex with either αGC or OCH may bind with altered affinity to the TCR, we stimulated NKT cells with plate-bound αGC-CD1d complexes instead of mAb to CD3 for the periods of time indicated in Figure 3B. Consistent with the previous results obtained with anti-CD3 stimulation, the level of IL-4 in the culture supernatant was increased after shorter periods of incubation. In contrast, IFN-γ was efficiently produced after longer incubation, showing that the short pulse of NKT cells with plate-bound αGC-CD1d complexes could recapitulate the OCH phenotype. These results demonstrate that the timing of the CD1d-lipid interaction rather than the "shape" of the OCH-CD1d complex is the decisive factor in controlling polarization of cytokine production by NKT cells.

Differential transcriptional properties of cytokine genes. To clarify the molecular basis for different kinetics of cytokine production by activated NKT cells, we next examined the effects of CsA or CHX on the NKT cell responses. Without any inhibitors, IL-4 production was more rapid and had a higher rate than IFN-γ production (Figure 3C), confirming the kinetic difference required for induction of each cytokine shown in Figure 3A. Production of both IL-4

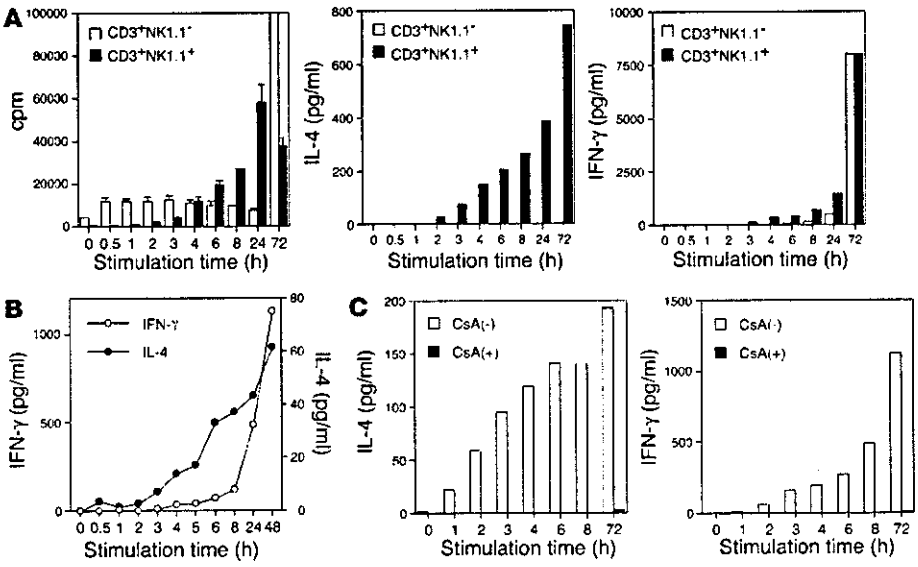

Figure 3

Kinetic analysis of NKT cell activation and cytokine production after glycolipid stimulation. (**A**) Differential production of IFN-γ and IL-4 by activated NKT cells. CD3+NK1.1+ NKT cells and conventional CD3+NK1.1− T cells were purified from liver mononuclear cells by cell sorting. The sorted cells were stimulated with immobilized mAb to CD3 for the time indicated on the *x* axis and were then removed and recultured on a fresh culture plate without anti-CD3 stimulation for up to 72 hours from the start of the anti-CD3 stimulation. Incorporation of [^{3}H]thymidine (1 μCi/well) during the final 16 hours of the culture was assessed (left), and culture supernatants were analyzed for the production of IL-4 (center) and IFN-γ (right) by ELISA. One experiment representative of three independent experiments with similar results is shown. (**B**) NKT cells purified from liver mononuclear cells were stimulated with plates coated with DimerX I loaded with αGC and were analyzed as shown in **A**. (**C**) NKT cells purified from liver mononuclear cells were stimulated as shown in **A** in the presence [CsA(+)] or absence [CsA(−)] of CsA (1 μg/ml). Culture supernatants were analyzed for the production of IL-4 and IFN-γ by ELISA.

and IFN-γ after TCR stimulation, however, was almost completely inhibited by pretreatment of NKT cells with CsA.

Similarly, CsA abolished the transcriptional activation of *IL-4* and *IFN-γ* genes in activated NKT cells (Figure 4A), indicating that TCR signal-induced activation of nuclear factor of activated T cell (NF-AT) is indispensable for the production of both cytokines by NKT cells. Meanwhile, transcription of these cytokine genes showed different sensitivities to CHX treatment (Figure 4A). Although transcriptional activation of *IL-4* was barely affected by CHX treatment, transcription of *IFN-γ* gene was almost completely blocked after treatment with CHX. These results indicate that transcriptional activation of *IFN-γ*, but not that of *IL-4*, requires de novo protein synthesis.

Next, we analyzed the sensitivities of other cytokine genes to CsA and CHX treatment (15–17). As shown in Figure 4B, transcriptional activation of all cytokine genes tested was completely blocked by pretreatment of NKT cells with CsA. Interestingly, transcription of the *IL-2* gene and *GM-CSF* gene were blocked by CHX treatment. In contrast, transcriptional activation of *TNF-α* was resistant to CHX treatment. These results indicate that cytokines produced by NKT cells could be divided into two groups based on their dependence on de novo protein synthesis.

Selective c-Rel induction after stimulation with αGC. Although NKT cells secrete a large number of cytokines upon stimulation, the regulatory mechanisms for the expression of each cytokine are still poorly understood. The susceptibility of IFN-γ production to CHX indicates that some newly synthesized protein(s) would promote specific transcription of the *IFN-γ* gene in NKT cells. To identify the protein responsible for αGC-induced transcription of the *IFN-γ* gene, we purified NKT cells from glycolipid-administered I-A^{b}β-deficient mice, which have two- to threefold higher numbers of NKT cells in the liver and the spleen than do wild-type B6 mice (18), and assessed NKT cell-derived total RNA by microarray analysis. As shown in Table 2, a number of cytokines and chemokines were differentially expressed after in vivo treatment with either αGC or OCH. It is noteworthy, however, that significant induction of *IFN-γ* transcription was observed only in αGC-treated samples, not in OCH-treated samples. Overall, the data obtained correlated well with previous results showing that OCH is a selective inducer of IL-4 production from NKT cells (9). There was no transcriptional upregulation of cytokines genes such as the *IFN-γ* and *IL-4* genes 12 hours after treatment with either glycolipid, indicating that NKT cells have undergone quiescence at this time point in the context of transcriptional upregulation of cytokine genes, although some genes are still upregulated.

Through analyzing the microarray data, we identified the protooncogene *c-Rel*, a member of the NF-κB family of transcription factors, as a candidate molecule that may play a role in the *IFN-γ* transcription. As shown in Figure 5A, *c-Rel* was inducibly expressed in NKT cells 1.5 hours after stimulation with αGC. In contrast, OCH treatment did not induce *c-Rel* transcription (Figure 5A). The transcription of other NF-κB family genes such as *p65/RelA* and *RelB* was not upregulated after treatment with αGC or OCH. Real-time PCR analysis also confirmed the selective induction of *c-Rel* after αGC stimulation (Figure 5B). CsA treatment inhibited *c-Rel* transcription, but CHX did not (Figure 5C), indicating that the inducible transcription of c-Rel is directly controlled by TCR signal–mediated activation of the NF-AT (19).

It is already known that c-Rel serves as a pivotal transcription factor for the Th1 response that would directly induce IFN-γ production in conventional T cells (20). However, very little is known about the function of this protooncogene in NKT cells during TCR-mediated activation. We therefore conducted time course analysis for transcriptional activation of *c-Rel* in parallel with *IL-4* and *IFN-γ*. We stimulated NKT cells with immobilized mAb to CD3 for 30–100 minutes and then cultured them without further stimulation for a total of 120 minutes. As shown in Figure 5D, *IFN-γ* expression was slightly downregulated in the first 90 minutes of TCR stimulation and was significantly upregulated when the cells were stimulated for 100 minutes. Interestingly, we found that the kinetics of *c-Rel* transcription were similar to those of *IFN-γ* transcription (Figure 5D, right). In contrast, transcrip-

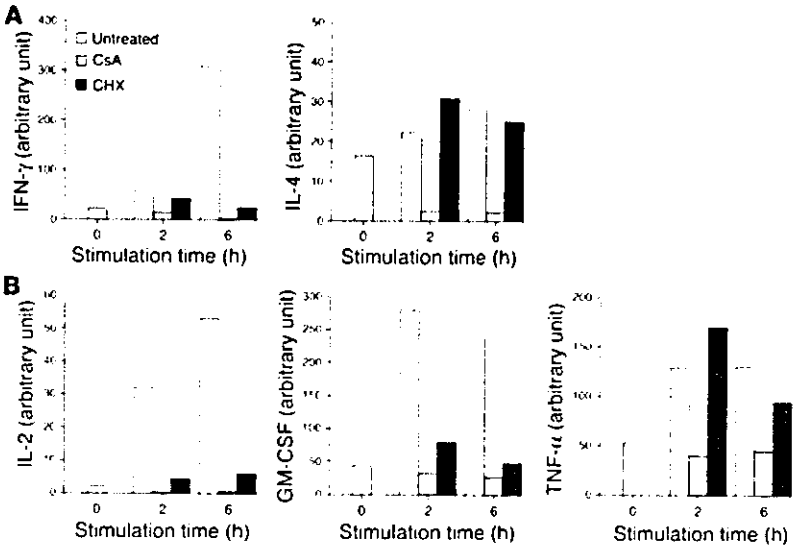

Figure 4
Differential sensitivity to CsA and CHX for transcriptional upregulation of *IFN-γ*, *IL-4*, and other cytokines. (**A**) Sorted NKT cells were pretreated with CsA (1 μg/ml) or with CHX (10 μg/ml) or without either reagent for 10 minutes and were then stimulated with immobilized mAb to CD3 for the indicated periods of time. Total RNA was extracted from each sample and analyzed for the relative amount of transcript of *IFN-γ* or *IL-4*. Data are presented as the amount of transcript in each sample relative to GAPDH. (**B**) Sorted NKT cells were pretreated with CsA (1 μg/ml) or with CHX (10 μg/ml) or without either reagent as shown in **A**. Total RNA was extracted from each sample and was analyzed for the relative amount of transcripts of *IL-2*, *GM-CSF*, or *TNF-α*. Data are presented as the relative amount of transcript in each sample.

tional activation of *IL-4* became evident 30 minutes after TCR stimulation and the transcript accumulated gradually in proportion to the duration of TCR stimulation. This result further confirmed that NKT cells require a longer TCR stimulus for IFN-γ expression.

Transcription of IFN-γ genes depends on c-Rel expression in NKT cells. To further investigate the functional involvement of c-Rel in the transcription of *IFN-γ* gene in NKT cells, we next examined whether forced expression of wild-type c-Rel or of its loss-of-function mutant could affect IFN-γ production by NKT cells. For this, we used bicistronic retroviral vectors expressing c-Rel along with GFP (pMIG/c-Rel) or a c-Rel dominant negative mutant that lacks the C-terminal transactivation domain but retains an intact Rel homology domain of c-Rel protein (pMIG/c-RelΔTA) (21) (Figure 6A). We infected liver-derived mononuclear cells with either retrovirus and stimulated sorted GFP-positive NKT cells with immobilized mAb to CD3 to analyze cytokine production. Retroviral transduction led to expression of GFP in approximately 10% of NKT cells (Figure 6B). Upon stimulation with mAb to CD3, GFP-positive cells from pMIG/c-Rel–infected cultures showed slightly augmented IFN-γ production compared with that of control pMIG-infected cells (Figure 6C). In contrast, GFP-positive cells from pMIG/c-RelΔTA–infected cultures secreted almost no IFN-γ after TCR stimulation (Figure 6C). These results demonstrate that inhibition of c-Rel function, via the introduction of a mutant form of c-Rel, abolishes IFN-γ production and that functional c-Rel is important for effective production of IFN-γ in activated NKT cells.

Discussion

In this study, we investigated the molecular mechanism for differential production of IFN-γ and IL-4 by activated NKT cells through a comparative analysis using the prototypic NKT cell ligands αGC and OCH. Treatment with αGC induced expression of both IFN-γ and IL-4 simultaneously, but OCH induced selective expression of IL-4 by NKT cells. Furthermore, we demonstrated that the CD1d-associated glycolipids with various lipid chain lengths showed different half-lives for NKT cell stimulation when applied in an endosome/lysosome-independent manner and induced the differential cytokine production by NKT cells in a lipid length–dependent manner. Accordingly, we demonstrated that IFN-γ production by NKT cells required longer TCR stimulation than did IL-4 production and depended on de novo protein synthesis. An NF-κB family transcription factor gene, the *c-Rel* gene, was inducibly transcribed in αGC-stimulated but not in OCH-stimulated NKT cells. Retroviral transduction of a loss-of-function mutant of c-Rel revealed the functional involvement of c-Rel in IFN-γ production by ligand-activated NKT cells. These results have provided a new interpretation of NKT cell activation — that the duration of TCR stimulation is critically influenced by the stability of each glycolipid ligand on CD1d molecules, which leads to the differential cytokine production by NKT cells.

We have previously demonstrated that administration of OCH consistently suppresses the development of EAE by inducing a Th2 bias in autoimmune T cells and that this Th2 shift is probably mediated by selective IL-4 production by NKT cells in vivo (9). Here we directly evaluated the cytokine profile of OCH-stimulated NKT cells using quantitative PCR analysis. Consistent with the previous assumption, NKT cells stimulated with OCH induced rapid production of IL-4 but led to only marginal induction of IFN-γ, confirming the presumed mechanism for the effect of OCH on EAE and CIA. As the "fold induction" of *IFN-γ* transcript after 1.5 hours of stimulation with αGC in microarray analysis was relatively low (fivefold for liver NKT cells and fourfold for spleen NKT cells) compared with the in vivo data, there are several possibilities to explain these results. First, quiescent transcripts of *IFN-γ* pre-existing in resting Vα14-invariant NKT cells (22) may raise the baseline of signal intensity in samples from untreated animals, resulting in a relative decrease in "fold induction" after glycolipid treatment. Second, detection of *IFN-γ* transcription in αGC-stimulated NKT cells might not be optimal, as injection of αGC induced a rapid elevation in IL-4 with the peak value at 2 hours and a delayed and prolonged elevation in IFN-γ in B6 mice (9). Third, αGC treatment significantly induces transcription of *CD154* (18.0-fold for αGC vs. 5.4-fold for OCH; data not shown), whose promoter has a functional NF-AT binding site and CD28 responsive element (CD28RE) (23, 24). Thus, augmented CD40/CD154 interaction may induce IL-12 expression by APCs, resulting in additional IFN-γ production (25). Finally, NKT cells are not necessarily the only source of IFN-γ after in vivo stimulation with αGC. The "serial" production of IFN-γ by NKT cells and NK cells has been demonstrated (6, 26). In particular, a C-glycoside analog of αGC has

Table 2
Differential gene expression patterns in αGC-treated and OCH-treated murine NKT cells

		Liver CD3⁺NK1.1⁺							Spleen CD3⁺NK1.1⁺						
		Untreated	αGC		OCH				Untreated	αGC		OCH			
Common name	GenBank		1.5 h		12 h		1.5 h		12 h		1.5 h		12 h		1.5 h		12 h	
IFN-γ	K00083	1.0	P	5.0	P	0.3	P	1.2	P	0.1	P	1.0	P	4.0	P	2.3	P	0.7	P	1.0	P
IL-2	m16762	1.0	A	391.4	P	1.2	A	12.3	P	1.3	A	1.0	A	23.4	P	0.2	A	1.0	A	0.3	A
IL-2	K02292	1.0	A	129.6	P	0.6	A	32.8	A	1.1	A	1.0	A	16.1	A	0.7	A	10.7	A	1.5	A
GM-CSF	X03020	1.0	P	38.0	P	0.4	A	4.1	P	0.1	A	1.0	A	15.7	P	1.4	A	2.7	A	2.1	A
IL-4	X03532	1.0	P	276.8	P	2.5	P	47.3	P	0.2	A	1.0	A	364.9	P	35.1	P	38.8	P	4.7	P
IL-4	M25892	1.0	P	38.2	P	0.2	P	7.7	P	0.1	A	1.0	P	69.6	P	7.6	P	9.1	P	1.1	P
IL-4	X03532	1.0	A	34.8	P	3.9	A	9.4	A	1.9	A	1.0	A	2.2	A	4.2	A	1.1	A	0.7	A
IL-13	M23504	1.0	A	993.0	P	1.4	A	56.1	P	1.8	A	1.0	A	140.7	P	12.3	A	19.1	A	2.3	A
TNF-α	D84196	1.0	P	30.8	P	2.1	P	1.7	P	1.2	P	1.0	P	16.5	P	2.5	P	1.8	P	2.6	P
Lymphotoxin A	M16819	1.0	P	6.9	P	0.2	A	1.4	P	0.1	A	1.0	P	2.5	P	1.7	P	1.2	P	0.9	P
IL-1α	M14639	1.0	P	25.1	P	5.6	P	3.1	P	4.4	P	1.0	P	6.7	P	5.8	P	1.1	P	2.7	P
IL-1β	M15131	1.0	P	8.0	P	9.8	P	1.3	P	7.9	P	1.0	P	3.3	P	2.2	P	0.6	P	1.5	P
*IL-1*RA	L32838	1.0	P	10.9	P	15.2	P	1.1	A	11.3	P	1.0	P	5.3	P	28.0	P	0.9	P	23.4	P
IL-3	K01668	1.0	A	33.2	P	2.6	A	4.7	A	1.2	A	1.0	A	4.0	A	1.1	A	1.4	A	1.7	A
IL-6	X54542	1.0	A	34.8	P	16.5	P	8.8	P	10.7	P	1.0	A	19.1	P	17.8	P	1.8	A	12.2	A

Real-time PCR analyses were conducted for *IFN-γ* and *IL-4* as well as for other selected cytokine genes listed in Figure 4 (data not shown) to confirm the correlation with those obtained from microarray analysis. Each probe was assigned a "call" of present (P; expressed) or "absent" (A; not expressed) using the Affymetrix decision matrix. GenBank, GenBank accession number; *IL-1*RA, *IL-1* receptor antagonist.

recently been shown to induce Th1-type activity superior to that induced by αGC, and IL-12 is indispensable for the Th1-skewing effect of the analog (27), indicating the importance of IL-12 in augmenting IFN-γ production in vivo (14, 28). Interestingly, the C-glycoside analog induces production of IFN-γ and IL-4 by NKT cells less strongly than does αGC at 2 hours after in vivo administration. Given that αGC and C-glycoside analog have the same structure for their lipid tails, they might be expected to have comparable affinity for CD1d molecules, and the slightly "twirled" α-anomeric galactose moiety between C-glycoside and O-glycoside may modulate the agonistic effect of these glycolipids. Furthermore, the C-glycoside is more resistant to hydrolysis in vivo and may have an advantage for effective production of IL-12 by APCs. In fact, OCH induces marginal IL-12 production after in vivo administration (data not shown), which makes it unable to induce IFN-γ production by various cells. Therefore, the beneficial feature of OCH as an immunomodulator is that it does not trigger production of IFN-γ in vivo.

As described previously, NKT cells recognize glycolipid antigens in the context of the nonpolymorphic MHC class I-like molecule CD1d (4). Crystal structure analysis revealed that the mouse CD1d molecule has a narrow and deep binding groove with extremely hydrophobic pockets, A′ and F′ (29). Thus the two aliphatic hydrocarbon chains would be captured by this binding groove of CD1d and the more hydrophilic galactose moiety of αGC or OCH would be presented to TCR on NKT cells. As OCH is an analog of αGC with a truncated sphingosine chain, it could be predicted that truncation of the hydrocarbon chain would make it more unstable on CD1d, which might then affect the duration of TCR stimulation on NKT cells. We demonstrated in this study that OCH detached from the CD1d molecule more rapidly than did αGC after a short-term pulse in which the glycolipids were segregated from the endosomal/lysosomal pathway. Accordingly, we showed that the initiation of IFN-γ production by NKT cells required more prolonged TCR stimulation than was required for IL-4 production. Methods such as surface plasmon resonance were not appropriate for direct assessment of the interaction between glycolipids and CD1d, possibly because of unpredictable micelle formation and the poor solubility of glycolipids in aqueous solvents (30). The half-life of the interaction of glycolipids and CD1d was reported to be less than 1 minute by surface plasmon resonance (31), contradicting functional assays suggesting a much longer half-life. Therefore, we applied a biological assay to evaluate the stability of these glycolipids on CD1d molecules, as described previously (13).

The characteristics of OCH are somewhat analogous to those of an altered peptide ligand (APL) that has been shown to induce a subset of functional responses observed in intact peptide and, in some cases, induce production of selected cytokines by T cells (32–34). Thus, OCH and possibly other αGC derivatives could be called "altered glycolipid ligands" (AGLs). Although the biological effects of APLs and AGLs could mediate a series of similar molecular events in target cells, it should be noted that APLs and AGLs differ in their "conceptual features." That is, APLs are usually altered in their amino acid residues to modify their affinity for TCRs, whereas AGLs have truncation of their hydrocarbon chain responsible for CD1d anchoring. This paper has highlighted the duration of NKT cell stimulation by CD1d-associated glycolipids as being a critical factor for determining the nature of AGLs for selective induction of cytokine production by NKT cells.

Given that IL-4 secretion consistently precedes IFN-γ production by NKT cells after TCR ligation, we speculated there were critical differences in the upstream transcriptional requirements for the *IFN-γ* and *IL-4* genes in NKT cells. In support of this speculation, CHX treatment specifically inhibited the transcription of *IFN-γ* but not that of *IL-4*. In contrast, transcription of both cytokines was abolished by CsA treatment, indicating that TCR-mediated activation of NF-AT is essential for the production of both cytokines. TCR signal-induced NF-AT activation occurs promptly corresponding to calcium influx (35). Meanwhile, the protein expression of specific

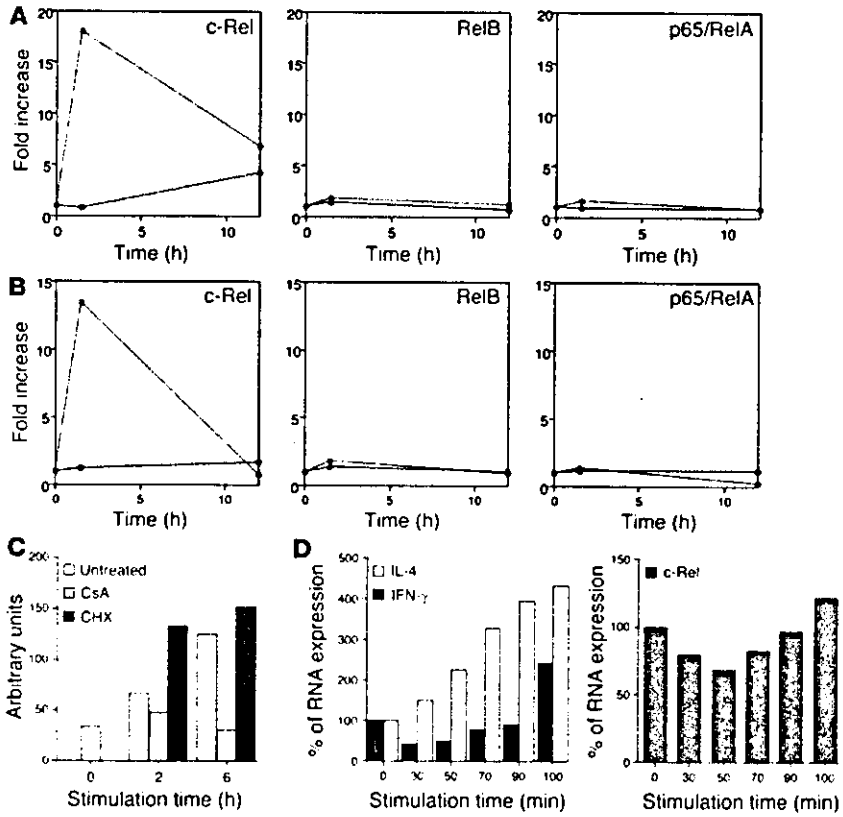

Figure 5
Induction of NF-κB family members in activated NKT cells. (**A**) Plotted values represent data of Affymetrix microarray analysis for the indicated genes. The αGC-stimulated (red lines) or OCH-stimulated (green lines) cells as well as unstimulated liver NKT cells were analyzed at the same time points and the data are presented as the relative value for stimulated NKT cells when the value in NKT cells derived from untreated animals was defined as 1. (**B**) Real-time PCR analysis for the same genes as in **A**. Data are presented as described in Figure 4. (**C**) Sorted liver NKT cells were pretreated with CsA or CHX and were stimulated with immobilized mAb to CD3, and comparative values of c-Rel transcripts relative to GAPDH were determined. (**D**) Sorted liver NKT cells were stimulated with immobilized mAb to CD3 for the indicated periods of time and then were cultured without stimulation for up to a total of 120 minutes after the initial stimulation. Total RNA was extracted from each sample and analyzed for relative amounts of transcripts of *IFN-γ* or *IL-4* (left), or *c-Rel* (right). The amount of RNA derived from unstimulated NKT cells was defined as 100%.

transcription factors takes more time to accomplish. The requirement for prolonged TCR stimulation for initiation of *IFN-γ* transcription may be due to its dependency on specific gene expression.

Recently, Matsuda et al. have shown using cytokine reporter mice that Vα14-invariant NKT cells express cytokine transcripts in the resting state, but express protein only after stimulation (22). We obtained a similar result with our microarray analysis, in that many cytokine transcripts including *IFN-γ* and *IL-4* were detectable in unstimulated NKT cells derived from liver or spleen, because most of them were assigned a "call" of "present" by the Affymetrix decision matrix, which means they were significantly expressed. The mechanism of translation of pre-existing cytokine transcripts after activation of NKT cells remains to be investigated.

Through microarray analysis and real-time PCR, we next identified a member of the NF-κB family of transcription factors, c-Rel, as being a protein rapidly expressed after αGC treatment and possibly responsible for the transcription of *IFN-γ*. Treatment with αGC selectively upregulated *c-Rel* transcription 1.5 hours after stimulation of NKT cells in vivo. OCH treatment, however, showed no induction of *c-Rel* transcription. Although *c-Rel* is transcriptionally upregulated after TCR stimulation of T cells (36), transcription of other NF-κB family members such as *p65/RelA*, *RelB*, *NF-κB1*, and *NF-κB2* was unchanged (data not shown). CsA treatment inhibited c-Rel transcription, but CHX did not, indicating that inducible transcription of c-Rel was directly controlled by TCR signal–mediated activation of NF-AT, which is consistent with a previous report (19). Although the pre-existing NF-κB proteins in general provide a means of rapidly altering cellular responses by inducing the destruction of IκB in order to enable NF-κB to be free for nuclear translocation and DNA binding, most of the nuclear c-Rel induced after T cell stimulation has been shown to be derived from newly translated c-Rel proteins. In contrast, pre-existing c-Rel scarcely translocates to the nucleus at all (36), indicating that the nuclear induction of c-Rel in T lymphocyte requires ongoing protein synthesis. The retrovirally transduced loss-of-function mutant c-Rel (c-RelΔTA) significantly inhibited transcription of *IFN-γ* genes, indicating the crucial role of c-Rel in their transcription after activation of NKT cells. Although it is possible that the Rel domain of the dominant negative mutant may affect a number of NF-κB dimers, it is unlikely, because IFN-γ production by stimulated NKT cells were CHX sensitive and other NK-κB members were not induced after stimulation in the microarray analysis. Retroviral transduction of wild-type c-Rel into NKT cells resulted in slightly augmented expression of IFN-γ after stimulation. Induction of endogenous c-Rel after in vitro stimulation might reduce the effect of retrovirally introduced c-Rel protein.

Whereas c-Rel has been associated with the functions of various cell types, its role in the immune system was first demonstrated in its involvement in *IL-2* transcription (37), in which it possibly induced chromatin remodeling of the promoter (38). Recently, the promoters for the genes encoding *IL-3*, *IL-5*, *IL-6*, *TNF-α*, *GM-CSF*, and *IFN-γ* were shown to contain κB sites or the κB-related CD28RE. Gene targeting of *c-Rel* in mice revealed that *c-Rel*–deficient T cells have a defect in the production of IL-2, IL-3, IL-5, GM-CSF, TNF-α, and IFN-γ, although expression of some of the cytokines was rescued by the addition of exogenous IL-2 (39, 40). Regarding the involvement of c-Rel in IFN-γ production, the c-Rel inhibitor pentoxyfylline (41) selectively suppresses Th1 cytokine production and EAE induction (42), and transgenic mice expressing the *trans*-dominant form of IκBα have a defect in IFN-γ production and the Th1 response (43). Recently, an elegant study using *c-Rel*–deficient mice revealed *c-Rel* has crucial roles in IFN-γ production by activated T cells and conse-

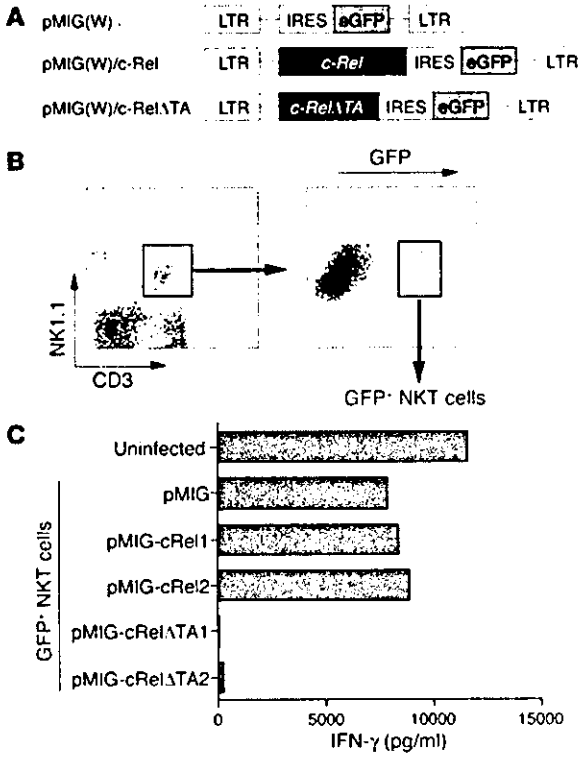

Figure 6
Cytokine production after retroviral transduction of c-Rel or c-RelΔTA into NKT cells. (**A**) DNA fragments encoding wild-type c-Rel or its mutant were cloned into the pMIG(W) bicistronic retrovirus vector. The mutant form of c-Rel (c-RelΔTA) lacks the transactivation domain of the c-Rel protein. LTR, long terminal repeat; IRES, internal ribosome entry site; eGFP, enhanced GFP. (**B**) Flow cytometric identification of cells transfected with the viral vector. Among the NK1.1+CD3+ liver NKT cells identified in the left panel, approximately 10% were GFP positive. The GFP-positive NKT cells were sorted for further analysis. (**C**) IFN-γ production by NKT cells transfected with c-Rel or its dominant negative mutant. The CD3+NK1.1+ NKT cells infected with the viruses were isolated based on their expression of GFP and were stimulated with immobilized mAb to CD3. For transduction of c-Rel or c-RelΔTA into NKT cells, two independent clones of each retroviral vector were used. The level of IFN-γ in the supernatants was measured by ELISA.

quent Th1 development by affecting the cellular functions of both T cells and APCs (20). Thus, the critical involvement of c-Rel for IFN-γ production in NKT cells is consistent with these findings.

Our results indicate that rapid calcium influx and subsequent NF-AT activation is essential for IFN-γ production by activated NKT cells and that c-Rel plays a crucial role in IFN-γ production as well. NF-AT shows quick and sensitive nucleocytoplasmic shuttling after TCR activation (35). Feske et al. demonstrated that the pattern of cytokine production by T cells was determined by the duration of nuclear residence of NF-AT (44) and that sustained NF-AT signaling promoted IFN-γ expression in CD4+ T cells (45). Considering the structural feature of αGC with longer lipid chain, sustained stimulation by αGC induces long-lasting calcium influx, resulting in sustained nuclear residence of NF-AT, and c-Rel protein synthesis, which enables NKT cells to produce IFN-γ. In contrast, the rather sporadic stimulation by OCH induces short-lived nuclear residence of NF-AT, followed by marginal c-Rel expression, which leaves NKT cells unable to produce IFN-γ (Figure 7). Thus, the kinetic and quantitative differences between αGC and OCH in the induction of transcription factors, such as NF-AT and c-Rel, determine the pattern of cytokine production by NKT cells. As CD1d molecules are nonpolymorphic and are remarkably well conserved among the species, the preferential induction of IL-4 production through NKT activa-

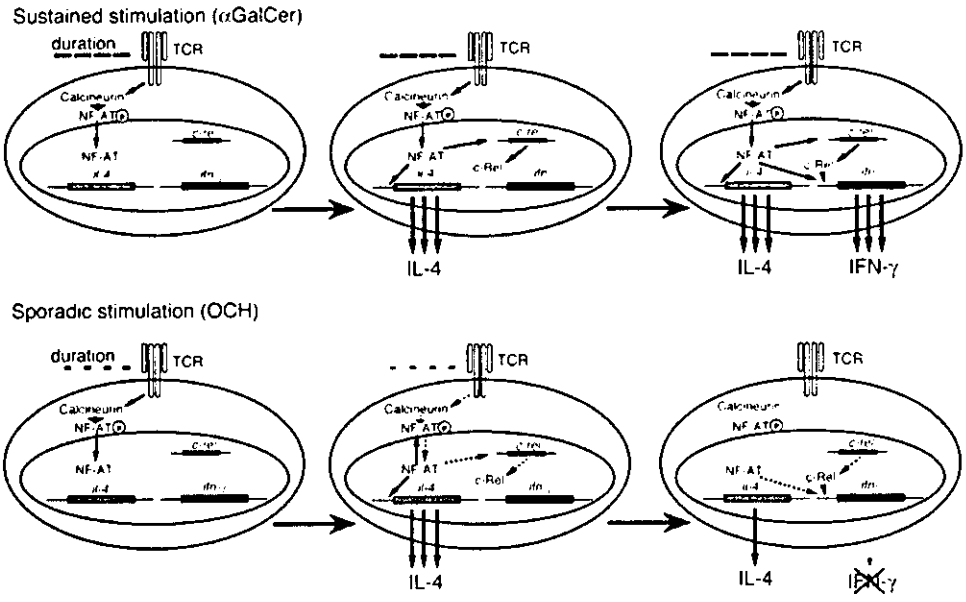

Figure 7
A model for the differential expression of IFN-γ and IL-4 after treatment of NKT cells with αGC or OCH. See text for details.

tion and subsequent Th2 polarization suggest that OCH may be an attractive therapeutic reagent to use for Th1-mediated autoimmune diseases such as multiple sclerosis and rheumatoid arthritis.

Acknowledgments

We thank Kyoko Hayakawa and Sebastian Joyce for providing the cell lines; Thomas Grundström for providing the c-Rel plasmid; and Luk Van Parijs for providing the retroviral vectors and packaging vector. We also thank Miho Mizuno and Chiharu Tomi for excellent technical assistance; and Yuki Kikai for cell sorting. We are grateful to John Ludvic Croxford for critical reading of the manuscript. This work was supported by the Organization for Pharmaceutical Safety and Research, Grant-in-Aid for Scientific Research (B) 14370169 from Japan Society for the Promotion of Science, Mochida Memorial Foundation, and Uehara Memorial Foundation.

Received for publication December 18, 2003, and accepted in revised form April 6, 2004.

Address correspondence to: Sachiko Miyake, Department of Immunology, National Institute of Neuroscience, NCNP, 4-1-1 Ogawahigashi, Kodaira, Tokyo 187-8502, Japan. Phone: 81-42-341-2711; Fax: 81-42-346-1753; E-mail: miyake@ncnp.go.jp.

1. Kronenberg, M., and Gapin, L. 2002. The unconventional lifestyle of NKT cells. *Nat. Rev. Immunol.* **2**:557–568.
2. Taniguchi, M., Harada, M., Kojo, S., Nakayama, T., and Wakao, H. 2003. The regulatory role of Vα14 NKT cells in innate and acquired immune response. *Annu. Rev. Immunol.* **21**:483–513.
3. Brossay, L., et al. 1998. CD1d-mediated recognition of an α-galactosylceramide by natural killer T cells is highly conserved through mammalian evolution. *J. Exp. Med.* **188**:1521–1528.
4. Kawano, T., et al. 1997. CD1d-restricted and TCR-mediated activation of vα14 NKT cells by glycosylceramides. *Science.* **278**:1626–1629.
5. Spada, F.M., et al. 1998. CD1d-restricted recognition of synthetic glycolipid antigens by human natural killer T cells. *J. Exp. Med.* **188**:1529–1534.
6. Carnaud, C., et al. 1999. Cross-talk between cells of the innate immune system: NKT cells rapidly activate NK cells. *J. Immunol.* **163**:4647–4650.
7. Fujii, S.I., Shimizu, K., Smith, C., Bonifaz, L., and Steinman, R.M. 2003. Activation of natural killer T cells by α-galactosylceramide rapidly induces the full maturation of dendritic cells in vivo and thereby acts as an adjuvant for combined CD4 and CD8 T cell immunity to a coadministered protein. *J. Exp. Med.* **198**:267–279.
8. Chiba, A., et al. 2004. Suppression of collagen-induced arthritis by natural killer T cell activation with OCH, a sphingosine-truncated analog of α-galactosylceramide. *Arthritis Rheum.* **50**:305–313.
9. Miyamoto, K., Miyake, S., and Yamamura, T. 2001. A synthetic glycolipid prevents autoimmune encephalomyelitis by inducing TH2 bias of natural killer T cells. *Nature.* **413**:531–534.
10. Burdin, N., et al. 1998. Selective ability of mouse CD1 to present glycolipids: α-galactosylceramide specifically stimulates Vα 14+ NK T lymphocytes. *J. Immunol.* **161**:3271–3281.
11. De Silva, A.D., et al. 2002. Lipid protein interactions: the assembly of CD1d1 with cellular phospholipids occurs in the endoplasmic reticulum. *J. Immunol.* **168**:723–733.
12. Antonsson, A., Hughes, K., Edin, S., and Grundstrom, T. 2003. Regulation of c-Rel nuclear localization by binding of Ca2+/calmodulin. *Mol. Cell. Biol.* **23**:1418–1427.
13. Moody, D.B., et al. 2002. Lipid length controls antigen entry into endosomal and nonendosomal pathways for CD1b presentation. *Nat. Immunol.* **3**:435–442.
14. Fujii, S., Shimizu, K., Kronenberg, M., and Steinman, R.M. 2002. Prolonged IFN-γ-producing NKT response induced with α-galactosylceramide-loaded DCs. *Nat. Immunol.* **3**:867–874.
15. Akbari, O., et al. 2003. Essential role of NKT cells producing IL-4 and IL-13 in the development of allergen-induced airway hyperreactivity. *Nat. Med.* **31**:31.
16. Heller, F., Fuss, I.J., Nieuwenhuis, E.E., Blumberg, R.S., and Strober, W. 2002. Oxazolone colitis, a Th2 colitis model resembling ulcerative colitis, is mediated by IL-13-producing NK-T cells. *Immunity.* **17**:629–638.
17. Leite-de-Moraes, M.C., et al. 2002. Ligand-activated natural killer T lymphocytes promptly produce IL-3 and GM-CSF in vivo: relevance to peripheral myeloid recruitment. *Eur. J. Immunol.* **32**:1897–1904.
18. Chen, H., Huang, H., and Paul, W.E. 1997. NK1.1+ CD4+ T cells lose NK1.1 expression upon in vitro activation. *J. Immunol.* **158**:5112–5119.
19. Venkataraman, L., Burakoff, S.J., and Sen, R. 1995. FK506 inhibits antigen receptor-mediated induction of c-rel in B and T lymphoid cells. *J. Exp. Med.* **181**:1091–1099.
20. Hilliard, B.A., et al. 2002. Critical roles of c-Rel in autoimmune inflammation and helper T cell differentiation. *J. Clin. Invest.* **110**:843–850. doi:10.1172/JCI200215254.
21. Carrasco, D., et al. 1998. Multiple hemopoietic defects and lymphoid hyperplasia in mice lacking the transcriptional activation domain of the c-Rel protein. *J. Exp. Med.* **187**:973–984.
22. Matsuda, J.L., et al. 2003. Mouse Vα14i natural killer T cells are resistant to cytokine polarization in vivo. *Proc. Natl. Acad. Sci. U. S. A.* **100**:8395–8400.
23. Tsytsykova, A.V., Tsitsikov, E.N., and Geha, R.S. 1996. The CD40L promoter contains nuclear factor of activated T cells-binding motifs which require AP-1 binding for activation of transcription. *J. Biol. Chem.* **271**:3763–3770.
24. Parra, E., Mustelin, T., Dohlsten, M., and Mercola, D. 2001. Identification of a CD28 response element in the CD40 ligand promoter. *J. Immunol.* **166**:2437–2443.
25. Kitamura, H., et al. 1999. The natural killer T (NKT) cell ligand α-galactosylceramide demonstrates its immunopotentiating effect by inducing interleukin (IL)-12 production by dendritic cells and IL-12 receptor expression on NKT cells. *J. Exp. Med.* **189**:1121–1128.
26. Smyth, M.J., et al. 2002. Sequential production of interferon-γ by NK1.1+ T cells and natural killer cells is essential for the antimetastatic effect of α-galactosylceramide. *Blood.* **99**:1259–1266.
27. Schmieg, J., Yang, G., Franck, R.W., and Tsuji, M. 2003. Superior protection against malaria and melanoma metastases by a C-glycoside analogue of the natural killer T cell ligand α-galactosylceramide. *J. Exp. Med.* **198**:1631–1641.
28. Brigl, M., Bry, L., Kent, S.C., Gumperz, J.E., and Brenner, M.B. 2003. Mechanism of CD1d-restricted natural killer T cell activation during microbial infection. *Nat. Immunol.* **4**:1230–1237.
29. Zeng, Z., et al. 1997. Crystal structure of mouse CD1: An MHC-like fold with a large hydrophobic binding groove. *Science.* **277**:339–345.
30. Cantu, C., 3rd, Benlagha, K., Savage, P.B., Bendelac, A., and Teyton, L. 2003. The paradox of immune molecular recognition of α-galactosylceramide: low affinity, low specificity for CD1d, high affinity for αβ TCRs. *J. Immunol.* **170**:4673–4682.
31. Benlagha, K., Weiss, A., Beavis, A., Teyton, L., and Bendelac, A. 2000. In vivo identification of glycolipid antigen-specific T cells using fluorescent CD1d tetramers. *J. Exp. Med.* **191**:1895–1903.
32. Evavold, B.D., and Allen, P.M. 1991. Separation of IL-4 production from Th cell proliferation by an altered T cell receptor ligand. *Science.* **252**:1308–1310.
33. Chaturvedi, P., Yu, Q., Southwood, S., Sette, A., and Singh, B. 1996. Peptide analogs with different affinities for MHC alter the cytokine profile of T helper cells. *Int. Immunol.* **8**:745–755.
34. Boutin, Y., Leitenberg, D., Tao, X., and Bottomly, K. 1997. Distinct biochemical signals characterize agonist- and altered peptide ligand-induced differentiation of naive CD4+ T cells into Th1 and Th2 subsets. *J. Immunol.* **159**:5802–5809.
35. Zhu, J., and McKeon, F. 2000. Nucleocytoplasmic shuttling and the control of NF-AT signaling. *Cell. Mol. Life Sci.* **57**:411–420.
36. Venkataraman, L., Wang, W., and Sen, R. 1996. Differential regulation of c-Rel translocation in activated B and T cells. *J. Immunol.* **157**:1149–1155.
37. Ghosh, P., Tan, T.H., Rice, N.R., Sica, A., and Young, H.A. 1993. The interleukin 2 CD28-responsive complex contains at least three members of the NF κ B family: c-Rel, p50, and p65. *Proc. Natl. Acad. Sci. U. S. A.* **90**:1696–1700.
38. Rao, S., Gerondakis, S., Woltring, D., and Shannon, M.F. 2003. c-Rel Is required for chromatin remodeling across the IL-2 gene promoter. *J. Immunol.* **170**:3724–3731.
39. Gerondakis, S., et al. 1996. Rel-deficient T cells exhibit defects in production of interleukin 3 and granulocyte-macrophage colony-stimulating factor. *Proc. Natl. Acad. Sci. U. S. A.* **93**:3405–3409.
40. Kontgen, F., et al. 1995. Mice lacking the c-rel proto-oncogene exhibit defects in lymphocyte proliferation, humoral immunity, and interleukin-2 expression. *Genes Dev.* **9**:1965–1977.
41. Wang, W., Tam, W.F., Hughes, C.C., Rath, S., and Sen, R. 1997. c-Rel is a target of pentoxifylline-mediated inhibition of T lymphocyte activation. *Immunity.* **6**:165–174.
42. Rott, O., Cash, E., and Fleischer, B. 1993. Phosphodiesterase inhibitor pentoxifylline, a selective suppressor of T helper type 1- but not type 2-associated lymphokine production, prevents induction of experimental autoimmune encephalomyelitis in Lewis rats. *Eur. J. Immunol.* **23**:1745–1751.
43. Aronica, M.A., et al. 1999. Preferential role for NF-κ B/Rel signaling in the type 1 but not type 2 T cell-dependent immune response in vivo. *J. Immunol.* **163**:5116–5124.
44. Feske, S., Draeger, R., Peter, H.H., Eichmann, K., and Rao, A. 2000. The duration of nuclear residence of NFAT determines the pattern of cytokine expression in human SCID T cells. *J. Immunol.* **165**:297–305.
45. Porter, C.M., and Clipstone, N.A. 2002. Sustained NFAT signaling promotes a Th1-like pattern of gene expression in primary murine CD4+ T cells. *J. Immunol.* **168**:4936–4945.

American Journal of Pathology, Vol. 165, No. 2, August 2004

The 14-3-3 Protein ε Isoform Expressed in Reactive Astrocytes in Demyelinating Lesions of Multiple Sclerosis Binds to Vimentin and Glial Fibrillary Acidic Protein in Cultured Human Astrocytes

Jun-ichi Satoh,* Takashi Yamamura,* and Kunimasa Arima†

From the Department of Immunology, National Institute of Neuroscience, and the Department of Neuropathology,† National Center Hospital for Mental, Nervous, and Muscular Disorders, National Center of Neurology and Psychiatry, Tokyo, Japan*

The 14-3-3 protein family consists of acidic 30-kd proteins expressed at high levels in neurons of the central nervous system. Seven isoforms form a dimeric complex that acts as a molecular chaperone that interacts with key signaling components. Recent studies indicated that the 14-3-3 protein identified in the cerebrospinal fluid of various neurological diseases including multiple sclerosis (MS) is a marker for extensive brain destruction. However, it remains unknown whether the 14-3-3 protein plays an active role in the pathological process of MS. To investigate the differential expression of seven 14-3-3 isoforms in MS lesions, brain tissues of four progressive cases were immunolabeled with a panel of isoform-specific antibodies. Reactive astrocytes in chronic demyelinating lesions intensely expressed β, ε, ζ, η, and σ isoforms, among which the ε isoform is a highly specific marker for reactive astrocytes. Furthermore, protein overlay, mass spectrometry, immunoprecipitation, and double-immunolabeling analysis showed that the 14-3-3 protein interacts with both vimentin and glial fibrillary acidic protein in cultured human astrocytes. These results suggest that the 14-3-3 protein plays an organizing role in the intermediate filament network in reactive astrocytes at the site of demyelinating lesions in MS. *(Am J Pathol 2004, 165:577–592)*

The 14-3-3 protein family consists of evolutionarily conserved, acidic 30-kd proteins originally identified by two dimensional analysis of brain protein extract.[1–4] Seven isoforms of the 14-3-3 protein named β, γ, ε, ζ, η, θ (also termed as τ), and σ have been identified in eukaryotic cells. Although the 14-3-3 protein is widely distributed in neural and nonneural tissues, it is expressed most abundantly in neurons in the central nervous system (CNS), where it represents 1% of total cytosolic proteins.[4–7] A homodimeric or heterodimeric complex, which is composed of the same or distinct isoforms of the 14-3-3 protein, constitutes a large cup-like structure with two ligand-binding sites in its groove. The dimeric complex acts as a novel molecular chaperone that interacts with key molecules involved in cell differentiation, proliferation, transformation, and apoptosis.[1–4] It regulates the function of target proteins by restricting their subcellular location, bridging them to modulate catalytic activity, and protecting them from dephosphorylation or proteolysis.[1–4,8–10] In general, the 14-3-3 protein binds to phosphoserine-containing motifs of the ligands such as RSXpSXP and RXY/FXpSXP in a sequence-specific manner.[1,3,10] More than 100 proteins have been identified as being 14-3-3 binding partners, including a range of intracellular signaling regulators such as Raf, BAD, protein kinase C (PKC), phophatidylinositol 3-kinase (PI3K), and cdc25 phosphatase.[1,4,8–10] Binding of the 14-3-3 protein to Raf is indispensable for Raf kinase activity in the Ras/MAPK signaling pathway, whereas 14-3-3 binding to the mitochondrial Bcl-2 family member BAD, when phosphorylated by a serine/threonine kinase Akt, inhibits apoptosis.[1–4] In addition to the phosphorylation-dependent interaction, the 14-3-3 protein can interact with a set of target proteins in a phosphorylation-independent manner.[10–12] The ε isoform binds to p190RhoGEF via a phosphoserine-independent interaction.[11]

Previous studies indicated that the 14-3-3 protein has isoform-specific and nonredundant functions.[1–4] Synaptic transmission and associative learning are impaired in

Supported by the Grant in Aid for Scientific Research (B2 15390280 and PA007 16017320); the Ministry of Education, Science, Sports, and Culture; and the Organization for Pharmaceutical Safety and Research, Kiko, Japan.

Accepted for publication April 22, 2004.

During submission of the present manuscript, an immunohistochemical study (Kawamoto Y, Akiguchi I, Kovács GG, Hicks H, Budka H: Increased 14-3-3 immunoreactivity in glial elements in patients with multiple sclerosis. Acta Neuropathol 2004, 107:137–143) has been published. This study showed that the 14-3-3 protein is expressed strongly in both astrocytes and oligodendrocytes in MS brains using an anti-14-3-3 protein antibody broadly reactive against all isoforms (H-8, sc-1657; Santa Cruz Biotechnology).

Supplemental information can be found on *http://www.amjpathol.org*.

Address reprint requests to Dr. Jun-ichi Satoh, Department of Immunology, National Institute of Neuroscience, NCNP, 4-1-1 Ogawahigashi, Kodaira, Tokyo 187-8502, Japan. E-mail: satoj@ncnp.go.jp.

Drosophila mutants lacking the ζ protein.[13] The 14-3-3 isoforms have distinct affinities for their target proteins. A preferential interaction is observed between PKCθ and the human 14-3-3θ isoform in T cells,[14] IGF1-receptor, IRS1, and ϵ isoform,[15] the apoptosis-inhibitor A20 and the human β and η isoforms,[16] and glucocorticoid receptor and the human η isoform.[17] The human β and ζ isoforms and not γ or ϵ isoforms interact with phosphorylated tau.[18] Furthermore, different isoforms show distinct patterns of spatial, temporal, and subcellular distribution. The human θ and σ isoforms are predominantly expressed in T cells and epithelial cells, respectively.[14,19] The rat ϵ and γ isoforms are enriched in the synaptosomal membranes,[20] and the γ isoform is the main 14-3-3 protein located in the Golgi apparatus in mammalian cells.[3] In the developing rat brain, defined populations of neurons express β, γ, ζ, and θ isoforms at specific stages of development.[6,7] In the adult mouse brain, β, γ, η, and ζ isoforms are widely distributed with the localization primarily in neurons, although some glial cells express ϵ, θ, and ζ isoforms.[21]

Recently, several lines of evidence have indicated that the 14-3-3 protein is involved in neurodegenerative processes. The 14-3-3 protein detected in the cerebrospinal fluid of Creutzfeldt-Jacob disease has been used as a biochemical marker for the premortem diagnosis of Creutzfeldt-Jacob disease in the context of differential diagnosis of progressive dementia.[22-24] In addition, intense immunoreactivity against the ζ isoform was identified in amyloid plaques in the Creutzfeldt-Jacob disease brain.[25] However, several studies including our own showed that the 14-3-3 protein is occasionally detectable in the cerebrospinal fluid of infectious meningoencephalitis, metabolic encephalopathy, cerebrovascular diseases, and multiple sclerosis (MS) presenting with severe myelitis, suggesting that it is not a marker specific for prion diseases but for extensive destruction of brain tissues causing the leakage of 14-3-3 protein into the cerebrospinal fluid.[4,22,26,27] In the Alzheimer's disease brain, neurofibrillary tangles express immunoreactivity against the 14-3-3 protein.[28] The 14-3-3ζ homodimer interacts with tau and glycogen synthase kinase-3β (GSK3β), and stimulates GSK3β-mediated tau phosphorylation.[29] In the Parkinson's disease brain, Lewy bodies possess γ, ϵ, ζ, and θ isoforms that interact with α-synuclein.[30,31] Dopamine-dependent neurotoxicity is mediated by a soluble complex composed of the 14-3-3 protein and α-synuclein, whose levels are markedly elevated in the substantia nigra of the Parkinson's disease brain.[32] The neurotoxicity of ataxin-1, the causative protein of spinocerebellar ataxia type 1, is enhanced by ϵ and ζ isoforms that bind to and stabilize ataxin-1 phosphorylated by Akt, thereby slowing its degradation.[33] Finally, expression of the θ isoform is enhanced in the spinal cord of amyotrophic lateral sclerosis.[34] However, it remains unknown whether the 14-3-3 protein plays an active role in the pathological process of MS.

In the present study, we investigated the differential expression of seven 14-3-3 isoforms in chronic active demyelinating lesions of MS. We found that reactive astrocytes intensely express β, ϵ, ζ, η, and σ isoforms, among which the ϵ isoform provides a specific marker to identify reactive astrocytes in the MS brain. Furthermore, the 14-3-3 protein interacts with vimentin and glial fibrillary acidic protein (GFAP) in cultured human astrocytes. These observations suggest that the 14-3-3 protein plays an organizing role in the intermediate filament (IF) network in reactive astrocytes at the site of demyelinating lesions in MS.

Materials and Methods

MS and Non-MS Brain Tissues

Ten-μ-thick tissue sections were prepared from the brain, spinal cord, and optic nerve derived from four autopsy cases of MS numbered 791, 744, 609, and 544. The clinical and neuroradiological profiles of these patients are shown in a supplementary table on The American

Table 1. The 14-3-3 Isoform-Specific or Broadly Reactive Antibodies Utilized for Immunochemistry and Western Blot Analysis

14-3-3 isoforms	Suppliers	Code	Antigen peptide	Origin	Specificity	Concentration used for immunohistochemistry (μg/ml)	Concentration used for Western blotting (μg/ml)
Pan	SC	sc-629	N-terminal	Rabbit	Reactive to all isoforms	0.4	0.04
Pan	SC	sc-1657	N-terminal	Mouse	Reactive to all isoforms	0.4	0.04
β	SC	sc-628	C-terminal	Rabbit	Reactive predominantly to β isoform, but crossreactive to other isoforms to a lesser extent	0.4	0.04
β	IBL	18641	N-terminal	Rabbit	Not crossreactive to other isoforms	2	1
γ	IBL	18647	C-terminal	Rabbit	Not crossreactive to other isoforms	5	0.2
ϵ	IBL	18643	C-terminal	Rabbit	Not crossreactive to other isoforms	2	1
ζ	IBL	18644	N-terminal	Rabbit	Not crossreactive to other isoforms	2	0.5
η	IBL	18645	N-terminal	Rabbit	Not crossreactive to other isoforms	5	1
θ (τ)	SC	sc-732	C-terminal	Rabbit	Not crossreactive to other isoforms	0.4	0.04
θ (τ)	IBL	10017	Recombinant, whole	Mouse	Mutually crossreactive to σ isoform	1	1
σ	IBL	18642	C-terminal	Rabbit	Not crossreactive to other isoforms	1	1

Abbreviations: SC, Santa Cruz Biotechnology; IBL, Immunobiological Laboratory. The specificity of the antibodies (IBL) is also shown on Supplementary Figure 1 at *http://www.amjpathol.org*.

Journal of Pathology website (*http://www.amjpathol.org*). The tissues were fixed with 4% paraformaldehyde (PFA) or 10% neutral formalin and embedded in paraffin. For the controls, tissue sections were prepared from the autopsied brains of six non-MS neurological and psychiatric disease cases that include a 47-year-old man with acute cerebral infarction who died of sepsis (no. 719), an 84-year-old man with acute cerebral infarction who died of disseminated intravascular coagulation (no. 786), a 62-year-old man with old cerebral infarction who died of pancreatic cancer (no. 789), a 56-year-old man with old cerebral infarction who died of myocardial infarction (no. 807), a 36-year-old woman with schizophrenia who died of lung tuberculosis (no. 523), and a 61-year-old man with schizophrenia who died of asphyxia (no. 826). In addition, they were prepared from the autopsied brains of six neurologically normal patients that include a 79-year-old woman who died of hepatic cancer (no. G6), a 75-year-old woman who died of breast cancer (no. G7), a 60-year-old woman who died of external auditory canal cancer (no. G8), a 74-year-old woman who died of gastric and hepatic cancers (no. G9), an 83-year-old woman who died of gastric cancer and myocardial infarction (no. A2623), and a 65-year-old man who died of liver cirrhosis and bronchopneumonia (no. A2647). Autopsies on all patients were performed at the National Center Hospital for Mental, Nervous, and Muscular Disorders, NCNP, Tokyo, Japan. Written informed consent was obtained in all cases.

Immunohistochemistry and Immunocytochemistry

After deparaffination, the tissue sections were heated by microwave at 95°C for 10 minutes in 10 mmol/L citrate sodium buffer (pH 6.0). They were then treated at room temperature for 15 minutes with 3% H_2O_2-containing methanol. For vimentin immunolabeling, the tissue sections were pretreated with 0.125% trypsin solution (Nichirei, Tokyo, Japan) at 37°C for 15 minutes. They were then incubated with 10% normal goat serum containing phosphate-buffered saline (PBS) at room temperature for 15 minutes to block nonspecific staining. The sections were incubated in a moist chamber at 4°C overnight with a panel of 14-3-3 isoform-specific antibodies or with antibodies broadly reactive against all isoforms listed in Table 1. The antibodies were obtained from Immunobiological Laboratory (IBL), Gumma, Japan, and Santa Cruz Biotechnology, Santa Cruz, CA. The specificity of the antibodies from IBL is shown in Supplementary Figure 1 on The American Journal of Pathology website, and additional information on those of Santa Cruz Biotechnology is available on the supplier's website (*www.scbt.com*). After washing with PBS, the tissue sections were labeled at room temperature for 30 minutes with peroxidase-conjugated secondary antibodies (Simple Stain MAX-PO kit, Nichirei) followed by incubation with a colorizing solution containing diaminobenzidine tetrahydrochloride and a counterstain with hematoxylin. To identify cell types expressing the 14-3-3 protein, adjacent sections were stained with the following antibodies: rabbit polyclonal antibody against GFAP (N1506; DAKO, Carpinteria, CA), rabbit polyclonal antibody against vimentin (H-84; Santa Cruz Biotechnology), mouse monoclonal antibody against vimentin (V9; Santa Cruz Biotechnology), rabbit polyclonal antibody against myelin basic protein (N1546; DAKO), mouse monoclonal antibody against CD68 (N1577; DAKO), and mouse monoclonal antibody against 70-kd and 200-kd neurofilament proteins (2F11; Nichirei). For negative controls, sections were incubated with a rabbit-negative control reagent (DAKO) instead of primary antibodies. The optimum concentrations of these antibodies and incubation periods were determined according to the supplier's instruction.

For double-labeling immunocytochemistry, cells on cover glasses were fixed with 4% PFA in 0.1 mol/L phos-

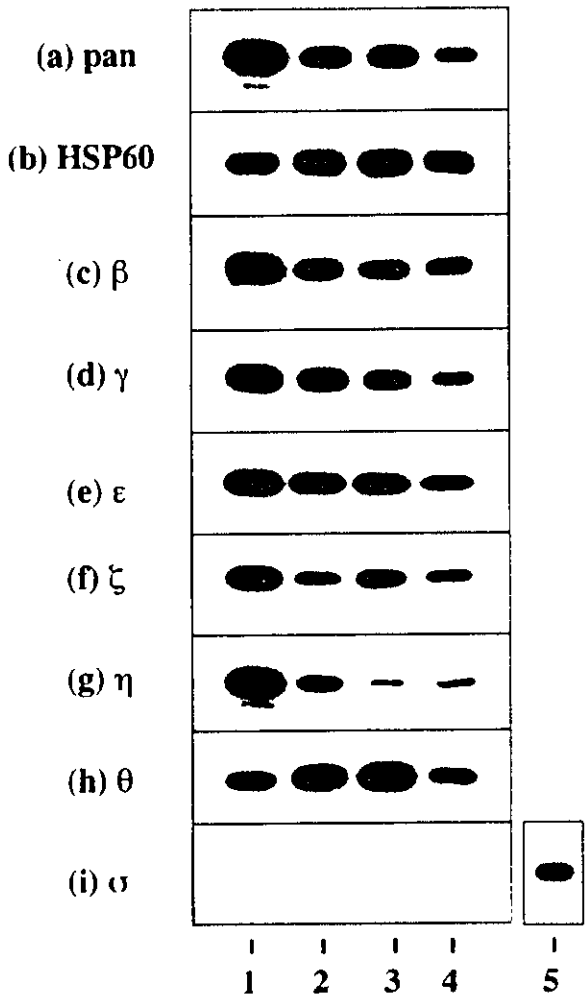

Figure 1. Constitutive expression of 14-3-3 isoforms in cultured human cells. Two μg of total protein extract isolated from brain tissues or cultured cells incubated in 10% FBS containing medium were processed for Western blot analysis using a battery of 14-3-3 isoform specific antibodies or the antibodies broadly reactive against all of the isoforms listed in Table 1, or the antibody against the housekeeping gene product HSP60. **a** to **i** indicate the following antibody specificity: **a**, all isoforms; **b**, HSP60; **c**, β; **d**, γ; **e**, ε; **f**, ζ; **g**, η; **h**, θ; and **i**, σ. **Lanes 1** to **4** represent homogenate of the human cerebrum (**lane 1**), NTera2 derived differentiated neurons (NTera2 N) (**lane 2**), U-373MG astrocytoma cells (**lane 3**), fetal human astrocytes (AST-F™) (**lane 4**), and HeLa cervical carcinoma cells (**lane 5**).

phate buffer (pH 7.4) at room temperature for 10 minutes, followed by incubation with PBS containing 0.5% Triton X-100 at room temperature for 20 minutes.[26] The cells were then incubated at room temperature for 30 minutes with a mixture of 14-3-3 isoform-specific antibody and rat monoclonal anti-GFAP antibody (2.2B10) or V9 antibody. Next, they were incubated at room temperature for 30 minutes with a mixture of rhodamine-conjugated anti-rabbit IgG and fluorescein isothiocyanate-conjugated anti-rat or mouse IgG (ICN-Cappel, Aurora, OH). After several washes, cover glasses were mounted on the slides with glycerol-polyvinyl alcohol, and the slides were examined under a Nikon ECLIPSE E800 universal microscope equipped with fluorescein and rhodamine optics. Negative controls were processed following these steps except for exposure to primary antibody.

Cell Culture

Two different sources of cultured human astrocytes were used. One was fetal human astrocytes named AS1477, provided by Drs K. Watabe and S. U. Kim of the University of British Columbia, Vancouver, BC, Canada. They were maintained in Dulbecco's modified Eagle's medium (DMEM) supplemented with 10% fetal bovine serum (FBS), 100 U/ml penicillin, and 100 μg/ml streptomycin (feeding medium). The other was astrocytes named AS-BW, whose differentiation was induced from neuronal progenitor (NP) cells. NP cells isolated from the brain of a human fetus at 18.5 weeks of gestation were obtained from BioWhittaker (Walkersville, MD). NP cells plated on a polyethyleneimine-coated surface were incubated in DMEM/F-12 medium containing an insulin-transferrin-selenium supplement (Invitrogen, Carlsbad, CA), 20 ng/ml recombinant human epidermal growth factor (Higeta, Tokyo, Japan), 20 ng/ml recombinant human basic fibroblast growth factor (PeproTech EC, London, UK), and 10 ng/ml recombinant human leukemia inhibitory factor (Chemicon, Temecula, CA) (NP medium).[35] For the induction of astrocyte differentiation, NP cells were incubated for several weeks in feeding medium instead of NP medium. This incubation induced vigorous proliferation and differentiation of astrocytes accompanied by a rapid reduction in nonastroglial cell types. Newborn mouse astrocytes were prepared as previously described.[26] In some experiments, cultured human and mouse astrocytes were plated at subconfluent density and incubated for 7 days in serum-free DMEM/F-12 medium supplemented with insulin-transferrin-selenium without inclusion of any other growth factors or in 10% FBS-containing DMEM/F-12 medium supplemented with insulin-transferrin-selenium.

Human cell lines such as U-373MG astrocytoma, NTera2 teratocarcinoma and HeLa cervical carcinoma were obtained from the RIKEN Cell Bank (Tsukuba, Japan) and the American Type Culture Collection (Rockville, MD). For the induction of neuronal differentiation, NTera2 cells maintained in the undifferentiated state (NTera2-U) were incubated for 4 weeks in feeding me-

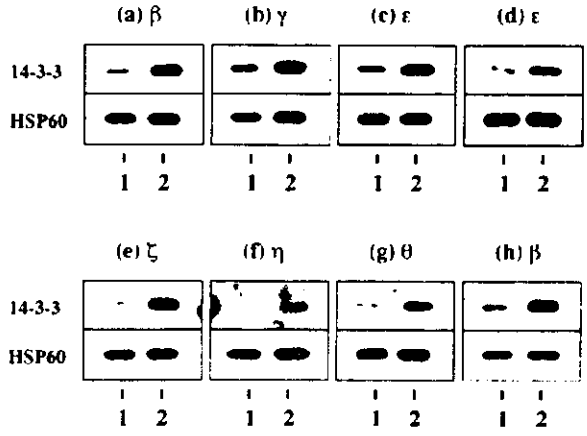

Figure 2. Growth dependent expression of various 14-3-3 isoforms in cultured human astrocytes. Human and mouse astrocytes were plated at subconfluent density and incubated for 7 days in the serum-free culture medium or in 10% FBS-containing culture medium. Two μg of total protein extract was processed for Western blot analysis using a battery of 14-3-3 isoform-specific antibodies or with the antibodies broadly reactive against all isoforms (**top**). After stripping the antibodies, identical blots were relabeled with the antibody against HSP60 for the standardization of expression levels (**bottom**). **a** to **g** (**top**) indicate the expression of β (**a**), γ (**b**), ε (**c**), ζ (**e**), η (**f**), and θ (**g**) in human astrocytes (AS1477); ε in human astrocytes (AS-BW) (**d**); and β in mouse astrocytes (**h**). **Lanes 1** and **2** represent the cells cultured under the serum-free growth arrested condition (**lane 1**) or the serum-containing growth promoting condition (**lane 2**). Additional data are shown in supplementary Figure 2 on the American Journal of Pathology website.

Table 2. Differential Expression of Seven 14-3-3 Isoforms in Glial Cells and Neurons in MS and Control Brains

Brains	Astrocytes			Microglia/macrophages			Oligodendrocytes			Neurons		
14-3-3 isoforms/cell types	MS	OND	NNC	MS	OND	NNC	MS	OND	NNC	MS	OND	NNC
β	maj(++)	maj(+)	no( )	maj(++)	maj(++)	no( )	min(+)	no( )	no( )	maj(++)	maj(++)	maj(++)
γ	min(++)	min(+)	no( )	min(++)	min(+)	no( )	no( )	no( )	no( )	maj(++)	maj(++)	maj(++)
ε	maj(++)	maj(++)	min(+)	no( )	no( )	no( )	no( )	no( )	no( )	min(+)	min(+)	min(+)
ζ	maj(++)	maj(++)	no( )	maj(++)	maj(++)	no( )	no( )	no( )	no( )	maj(++)	maj(++)	maj(++)
η	maj(++)	maj(++)	no( )	maj(++)	min(++)	no( )	no( )	no( )	no( )	maj(++)	maj(++)	maj(++)
θ	min(+)	min(+)	no( )	no( )	no( )	no( )	min(++)	min(++)	min(+)	min(+)	min(+)	min(+)
σ	min(++)	min(++)	min(+)	no( )	no( )	no( )	no( )	no( )	no( )	no( )	no( )	no( )

The present study includes four MS cases numbered #791, 744, 609, and 544 whose clinical profiles are given in a supplementary table on the AJP website, six non-MS neurological and psychiatric disease cases (OND) composed of #719 acute cerebral infarction, #786 acute cerebral infarction, #789 old cerebral infarction, #807 old cerebral infarction, #523 schizophrenia, and #826 schizophrenia, and six neurologically normal cases (NNC) composed of #G6, #G7, #G8, #G9, #A2623, and #A2647, whose profiles are described in the Materials and Methods section.

The population size of the immunoreactive cells is expressed as maj, major (large) population; min, minor (small) population; and no, almost no population. The intensity of immunoreactivity is graded as ( ) negative, (+) weak, and (++) intense.

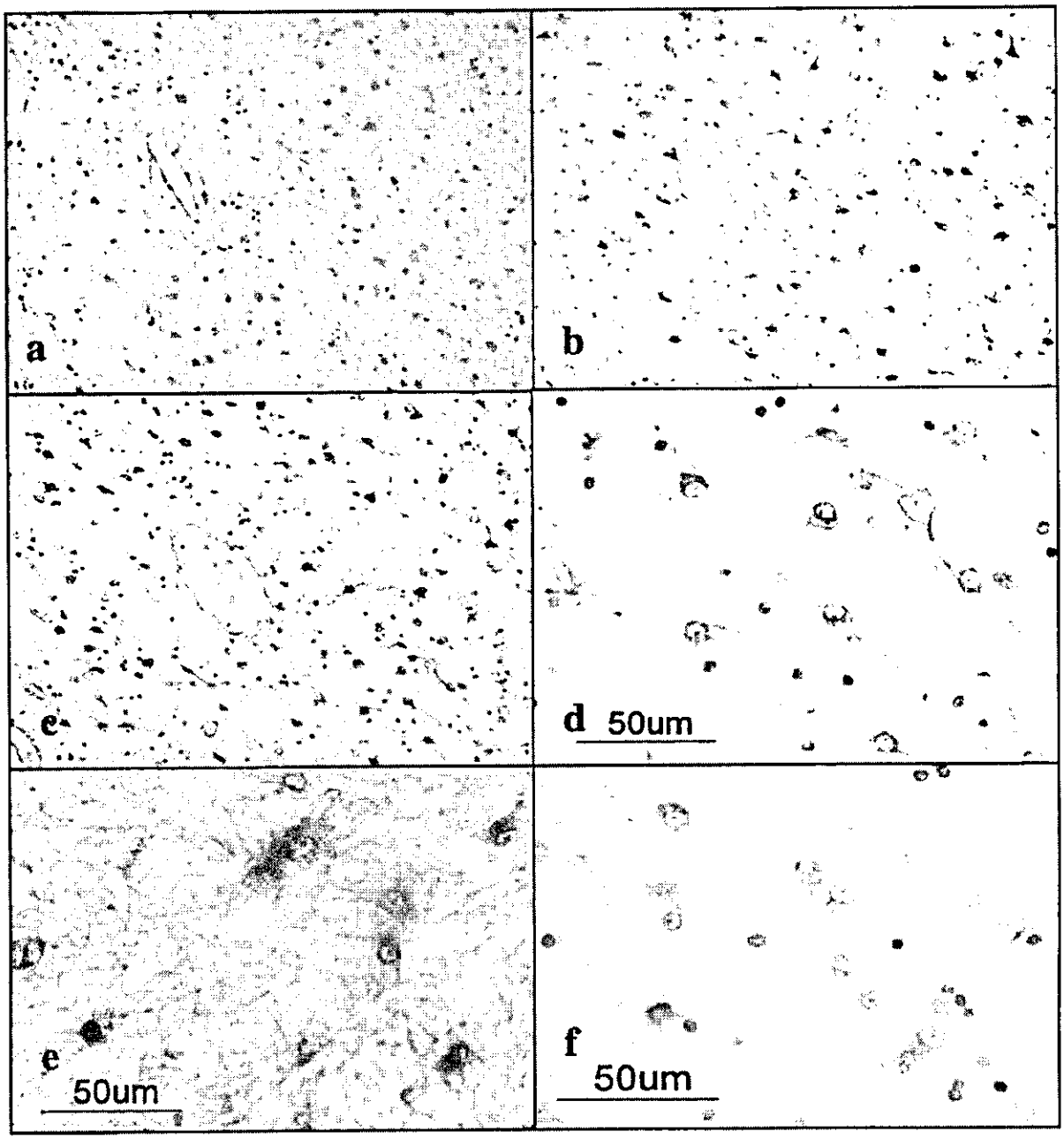

Figure 3. The 14-3-3ε isoform is expressed in reactive astrocytes in chronic demyelinating lesions of MS. MS brain tissues were processed for immunohistochemical analysis using ε isoform specific antibody or the antibody against GFAP or vimentin. **a** to **f** represent the following: **a:** no. 744 MS, chronic active demyelinating lesions in the subcortical white matter of the frontal lobe (H&E). **b:** No. 744 MS, the area corresponding to **a** (GFAP). Many reactive astrocytes are stained. **c:** No. 744 MS, the area corresponding to **a** (ε). Many reactive astrocytes are stained. **d:** No. 744 MS, a higher magnification view of **c** (ε). Reactive astrocytes are stained. **e:** No. 541 MS, chronic inactive demyelinating lesions in the optic nerve (ε). Reactive astrocytes and the glial scar are stained. **f:** No. 744 MS, chronic active demyelinating lesions in the subcortical white matter of the frontal lobe (vimentin). Reactive astrocytes are stained.

dium containing 10^{-6} mol/L *all trans* retinoic acid (Sigma, St. Louis, MO), replated twice and then plated on a surface coated with Matrigel Basement Membrane Matrix (Becton Dickinson, Bedford, MA). They were incubated for another 2 weeks in feeding medium containing a cocktail of mitotic inhibitors, resulting in the enrichment of differentiated neurons (NTera2-N).[36]

Western Blot Analysis

To prepare total protein extract for Western blot analysis, the cells and tissues were homogenized in RIPA lysis buffer composed of 50 mmol/L Tris-HCl (pH 7.5), 150 mmol/L NaCl, 1% Nonidet P-40, 0.5% sodium deoxycholate, 0.1% sodium dodecyl sulfate (SDS), and a cock-

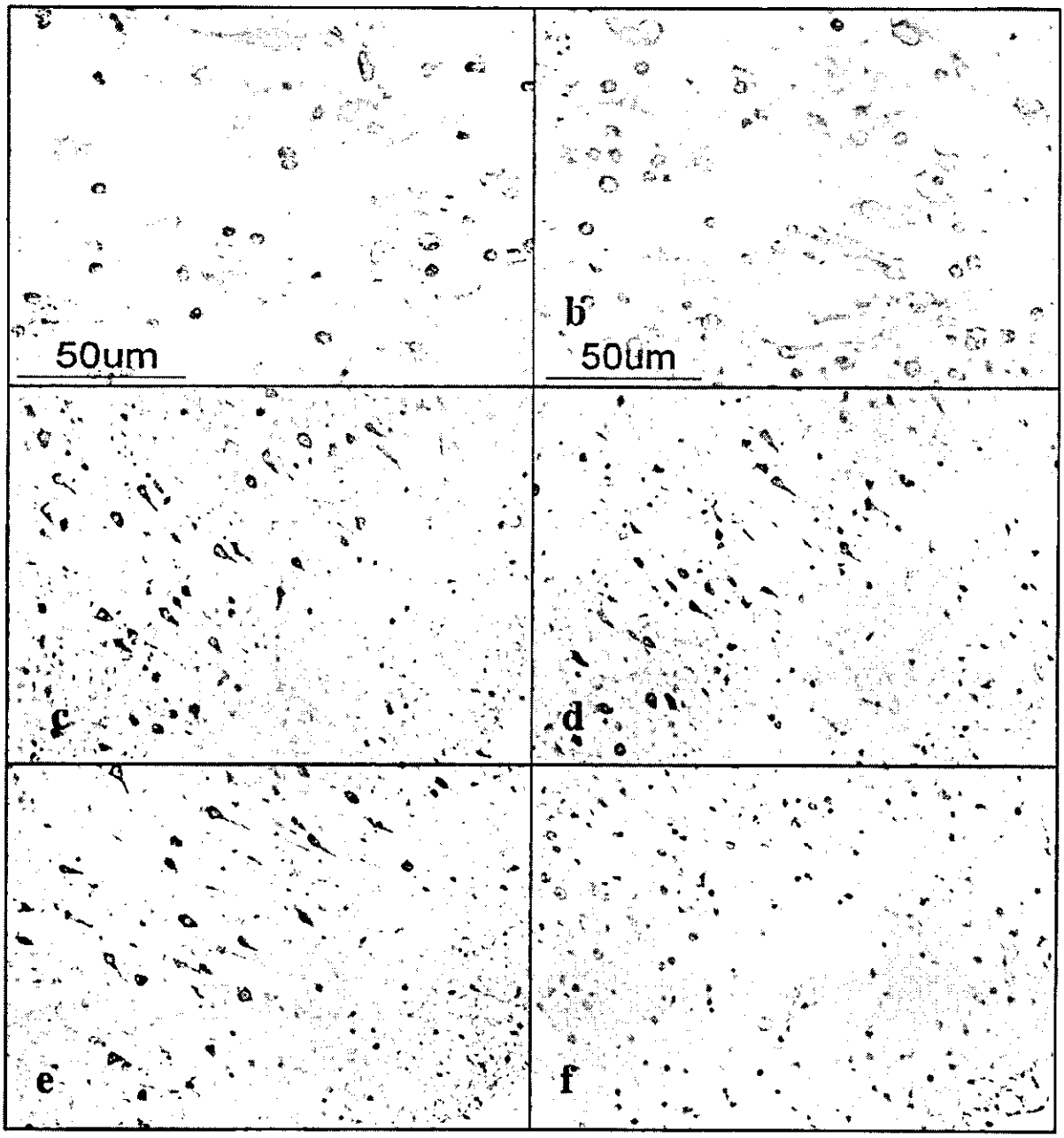

Figure 4. Expression of various 14-3-3 isoforms in reactive astrocytes and cortical neurons in MS brain. MS brain tissues were processed for immunohistochemical analysis using a battery of 14-3-3 isoform specific antibodies. **a** to **f** represent the following: **a:** no. 744 MS, chronic active demyelinating lesions in the subcortical white matter of the frontal lobe (β). Reactive astrocytes are stained. **b:** No. 744 MS, chronic active demyelinating lesions in the subcortical white matter of the frontal lobe (ζ). Reactive astrocytes are stained. **c:** No. 744 MS, the cerebral cortex of the frontal lobe (γ). Cortical neurons are stained. **d:** No. 744 MS, the area corresponding to **c** (η). Cortical neurons are stained. **e:** No. 744 MS, the area corresponding to **c** (ζ). Cortical neurons are stained. **f:** No. 744 MS, the area corresponding to **c** (ε). Cortical neurons are devoid of staining.

tail of protease inhibitors (Roche Diagnositics, Mannheim, Germany), followed by centrifugation at 12,000 rpm at room temperature for 20 minutes. The supernatant was collected for separation on a 12% SDS-polyacrylamide gel electrophoresis (PAGE) gel and the protein concentration was determined by a Bradford assay kit (Bio-Rad, Hercules, CA). After gel electrophoresis, the protein was transferred onto nitrocellulose membranes and immunolabeled at room temperature overnight with a panel of anti-14-3-3 protein antibodies listed in Table 1. Then, the membranes were incubated at room temperature for 30 minutes with horseradish peroxidase-conjugated anti-rabbit IgG or anti-mouse IgG (Santa Cruz Biotechnology). The specific reaction was visualized with a Western blot detection system using a chemiluminescent substrate (Pierce, Rockford, IL). After the antibodies were stripped

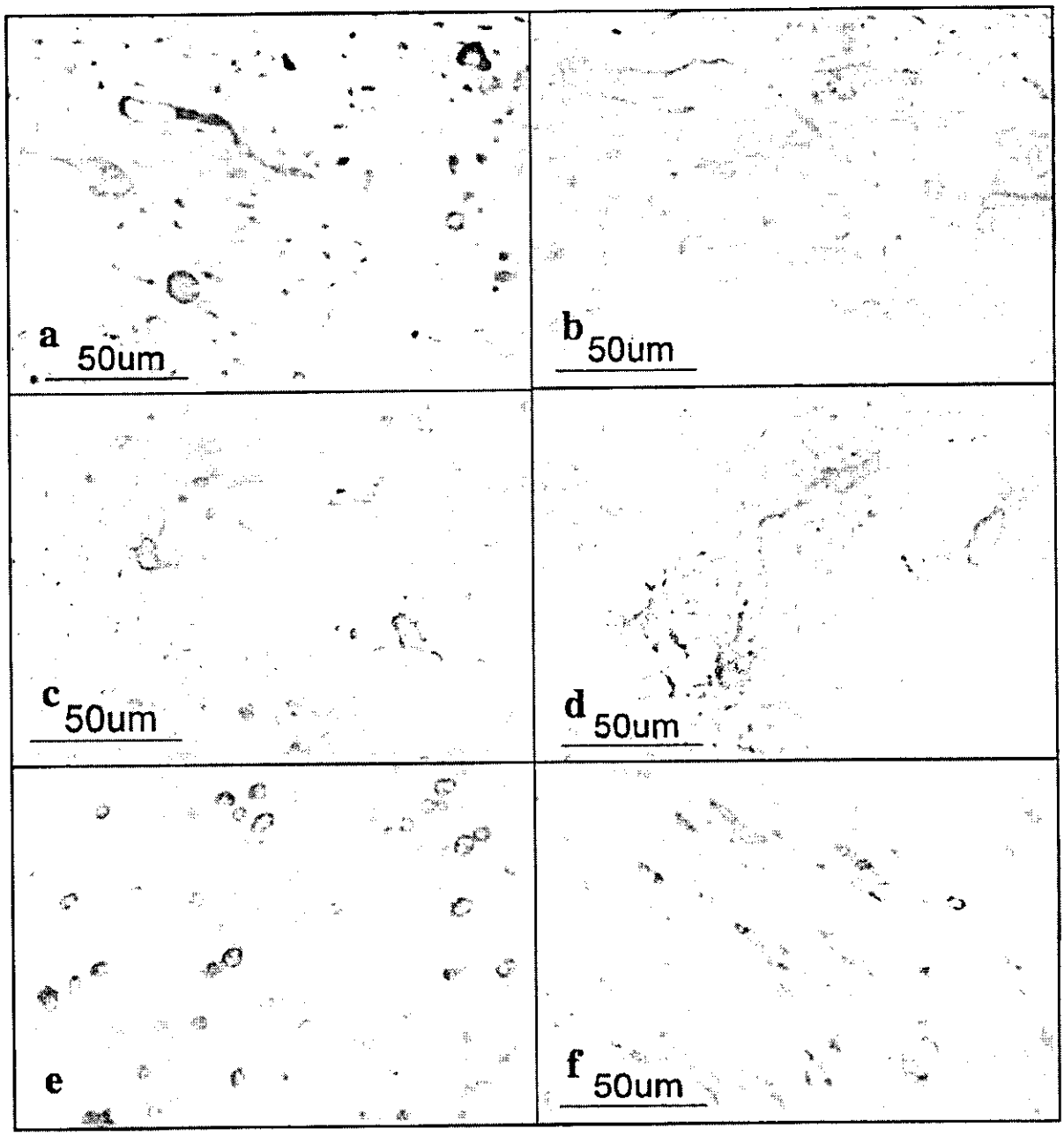

Figure 5. Expression of various 14-3-3 isoforms in reactive astrocytes, surviving oligodendrocytes, and injured axons in chronic demyelinating lesions of MS and in infarcted lesions. The brains of MS and non-MS control cases were processed for immunohistochemical analysis using a battery of 14-3-3 isoform specific antibodies. **a** to **f** represent the following: **a:** no. 609 MS, chronic active demyelinating lesions in the medulla oblongata (×). Disrupted axons are stained. **b:** No. 749 acute cerebral infarction, infarcted lesions in the parietal cerebral cortex (×). Reactive astrocytes are stained. **c:** No. 791 MS, chronic inactive lesions in the pons (×). Reactive astrocytes are stained. **d:** No. 749 acute cerebral infarction, infarcted lesions in the parietal cerebral cortex (×). Reactive astrocytes are stained. **e:** No. 609 MS, chronic active demyelinating lesions in the periventricular white matter of the frontal lobe (×). Surviving oligodendrocytes are stained. **f:** No. 744 MS, chronic active demyelinating lesions in the optic nerve (×). Surviving oligodendrocytes are stained.

by incubating the membranes at 50°C for 30 minutes in stripping buffer composed of 62.5 mmol/L Tris-HCl (pH 6.7), 2% SDS, and 100 mmol/L 2-mercaptoethanol, the membranes were processed for relabeling with goat polyclonal antibody against human heat shock protein HSP60 (N-20; Santa Cruz Biotechnology) followed by incubation with horseradish peroxidase-conjugated anti-goat IgG (Santa Cruz Biotechnology). Densitometric analysis was performed using NIH image version 1.61 software to quantify the intensity of the immunoreactive bands.[36]

Immunoprecipitation Experiments

To prepare total protein extract for immunoprecipitation experiments, the cells were homogenized in M-PER lysis buffer (Pierce) with a cocktail of protease inhibitors fol-

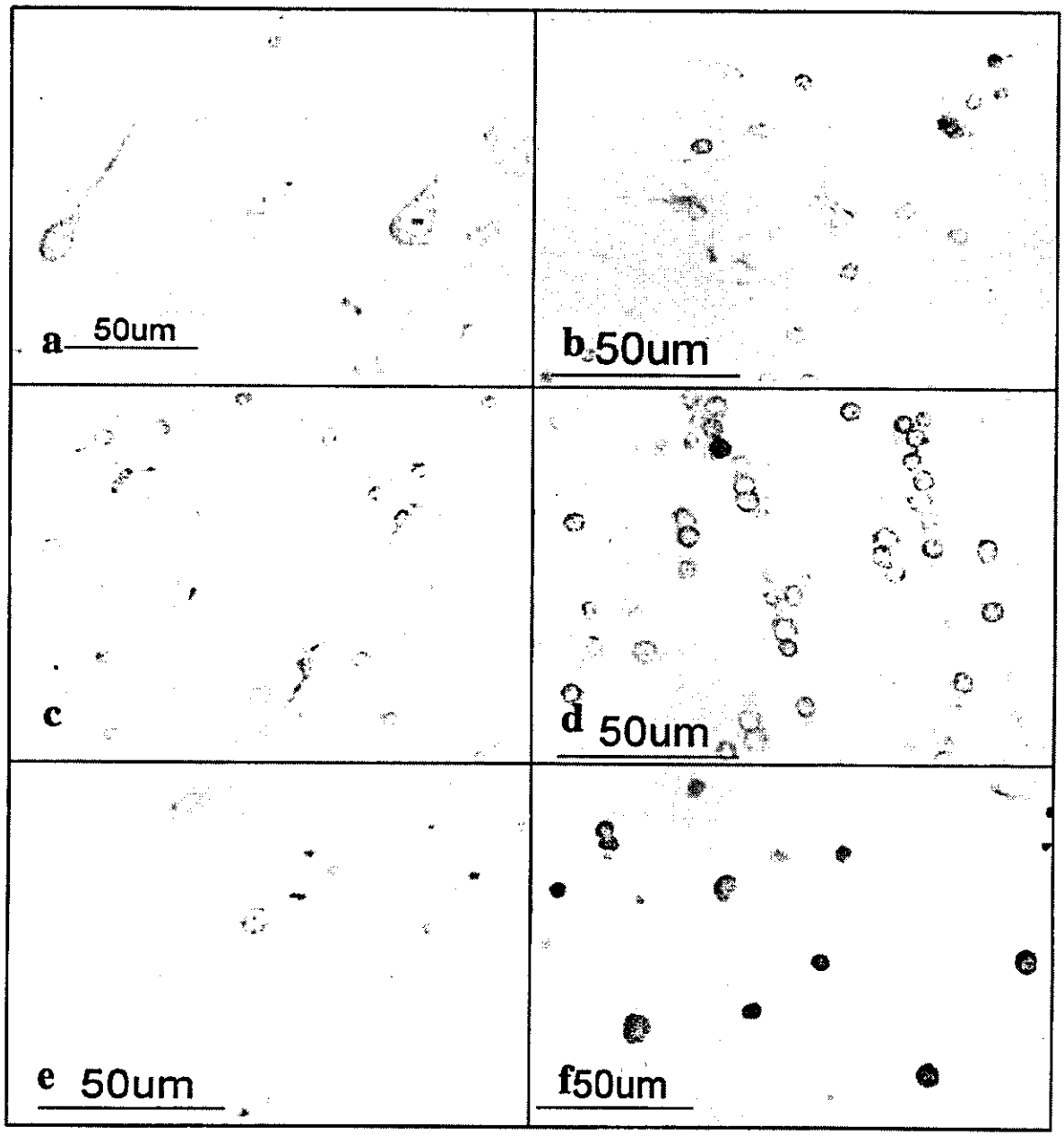

Figure 6. Expression of various 14-3-3 isoforms in neurons, astrocytes, oligodendrocytes, and microglia in non-MS brains. The brains of non-MS control cases were processed for immunohistochemical analysis using a battery of 14-3-3 isoform specific antibodies. **a** to **f** represent the following: **a:** no. 69 neurologically normal subject, the frontal cerebral cortex (×). Cortical neurons are stained. **b:** No. 523 schizophrenia, frontal cerebral cortex (×). Astrocytes are stained. **c:** No. 826 schizophrenia, the frontal cerebral cortex (×). Microglia are stained. **d:** No. 786 acute cerebral infarction, the subcortical white matter of the parietal lobe (×). Surviving oligodendrocytes are stained. **e:** No. 67 neurologically normal subject, the frontal cerebral cortex (×). A few astrocytes are stained. **f:** No. 789 old cerebral infarction, the frontal cerebral cortex (×). The nuclei of reactive astrocytes are stained.

lowed by centrifugation at 12,000 rpm at room temperature for 20 minutes. After preclearance, the supernatant was incubated at 4°C for 1 hour with a panel of anti-14-3-3 protein antibodies or the same amount of normal rabbit IgG (Santa Cruz Biotechnology). It was then incubated with Protein G Sepharose (Amersham Bioscience, Piscataway, NJ). After several washes, the immunoprecipitates were processed for Western blot analysis using V9 antibody or mouse monoclonal antibody against GFAP (GA5; Nichrei).

Two-Dimensional Gel Electrophoresis and Mass Spectrometry Analysis

To prepare total protein extract for two-dimensional gel electrophoretic analysis, the cells were homogenized in

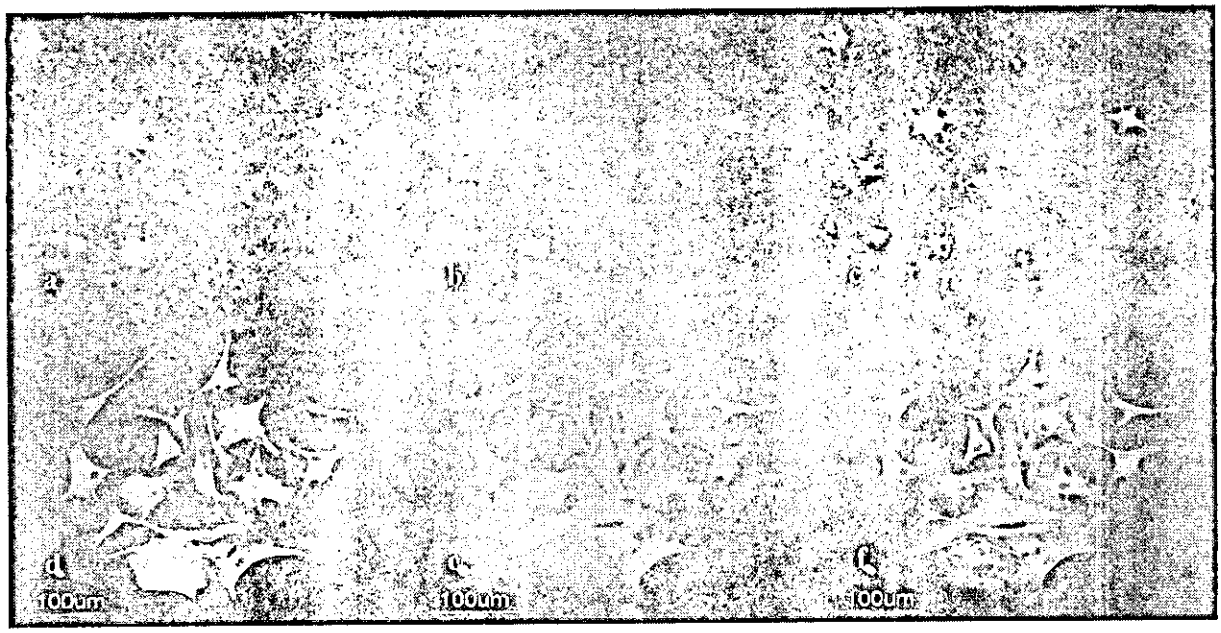

Figure 7. Co-expression of the 14-3-3ε isoform and GFAP in reactive astrocytes in chronic demyelinating lesions of MS and in cultured human astrocytes. Cultured human astrocytes and MS brain tissues were processed for double immunolabeling with anti GFAP antibody and ε isoform specific antibody followed by labeling with fluorescein isothiocyanate- and rhodamine-conjugated secondary antibodies. **a** to **f** represent no. 7-11, chronic active demyelinating lesions in the subcortical white matter of the frontal lobe (**a**–**c**), cultured human astrocytes (AS-BW-1) (**d**–**f**). GFAP (**a**, **d**), ε (**b**, **e**), and the overlay (**c**, **f**).

rehydration buffer composed of 8 mol/L urea, 2% CHAPS, 0.5% carrier ampholytes (pH 4 to 6), 20 mmol/L dithiothreitol, 0.002% bromophenol blue, and a cocktail of protease inhibitors and phosphatase inhibitors (Sigma). Urea-soluble protein was separated by isoelectric focusing using the ZOOM IPGRunner system (Invitrogen) loaded with an immobilized pH 4.5 to 5.5 gradient strip. After the first dimension of isoelectric focusing, the protein was separated in the second dimension on a NuPAGE 4 to 12% polyacrylamide gel (Invitrogen). The gel was stained using Coomassie brilliant blue G-250 solution or the Silverquest silver staining kit (Invitrogen). It was transferred onto a polyvinylidene difluoride membrane for protein overlay and Western blot analysis. Spots of interest were excised from the gels, trypsinized, and processed for mass spectrometry (nanoESI-MS/MS) analysis followed by database searching using MASCOT software (Invitrogen Proteome, Yokohama, Japan).

Protein Overlay Analysis

To prepare the 14-3-3 protein-specific probe for protein overlay analysis, the open reading frame of the human 14-3-3ε isoform gene (YWHAE, GenBank accession No. NM_006761) was amplified from the cDNA of NTera2-N cells by the polymerase chain reaction using sense and anti-sense primers (5′atggatgatcgagaggatctggtg3′ and 5′tcactgattttcgtcttccacgtc3′). The polymerase chain reaction product was cloned into a prokaryotic expression vector pTrcHis-TOPO (Invitrogen). The expression of recombinant human 14-3-3ε protein having an N-terminal Xpress tag for detection (rh14-3-3ε) was induced in *Escherichia coli* by exposure to isopropyl β-thiogalactoside. The recombinant protein was further purified through a HiTrap chelating HP column (Amersham Bioscience) and by separation on a 12% SDS-PAGE gel. Recombinant human interferon-stimulated protein ISG15 fused to an N-terminal Xpress tag (rhISG15), a vimentin-binding protein in human cancer cells,[17] was prepared for the control probe. The polyvinylidene difluoride membrane on which the gel was blotted was incubated at room temperature overnight with 1 μg/ml rh14-3-3ε or rhISG15 probe, followed by immunolabeling with mouse monoclonal anti-Xpress antibody (Invitrogen) and horseradish peroxidase-conjugated anti-mouse IgG. After the probes and antibodies were stripped by incubating the membrane at 50°C for 30 minutes in stripping buffer, it was repeatedly relabeled with V9 antibody, GA5 antibody, or rabbit polyclonal antibodies specific for phosphorylated Ser-39, Ser-72, or Ser-83 epitopes of vimentin (Santa Cruz Biotechnology), followed by incubation with horseradish peroxidase-conjugated anti-mouse or rabbit IgG.

Results

Growth-Dependent Expression of 14-3-3 Isoforms in Cultured Human Astrocytes

To investigate the expression pattern of seven 14-3-3 isoforms in human neural cells, cultured human astrocytes, NTera2-N neurons, and U-373MG astrocytoma cells, all of which were incubated in 10% FBS-containing culture medium, were processed for Western blot analysis using a panel of isoform-specific antibodies or the antibodies broadly reactive against all of the isoforms listed in Table 1. Cultured human astrocytes, neurons, and astrocytoma cells, along with

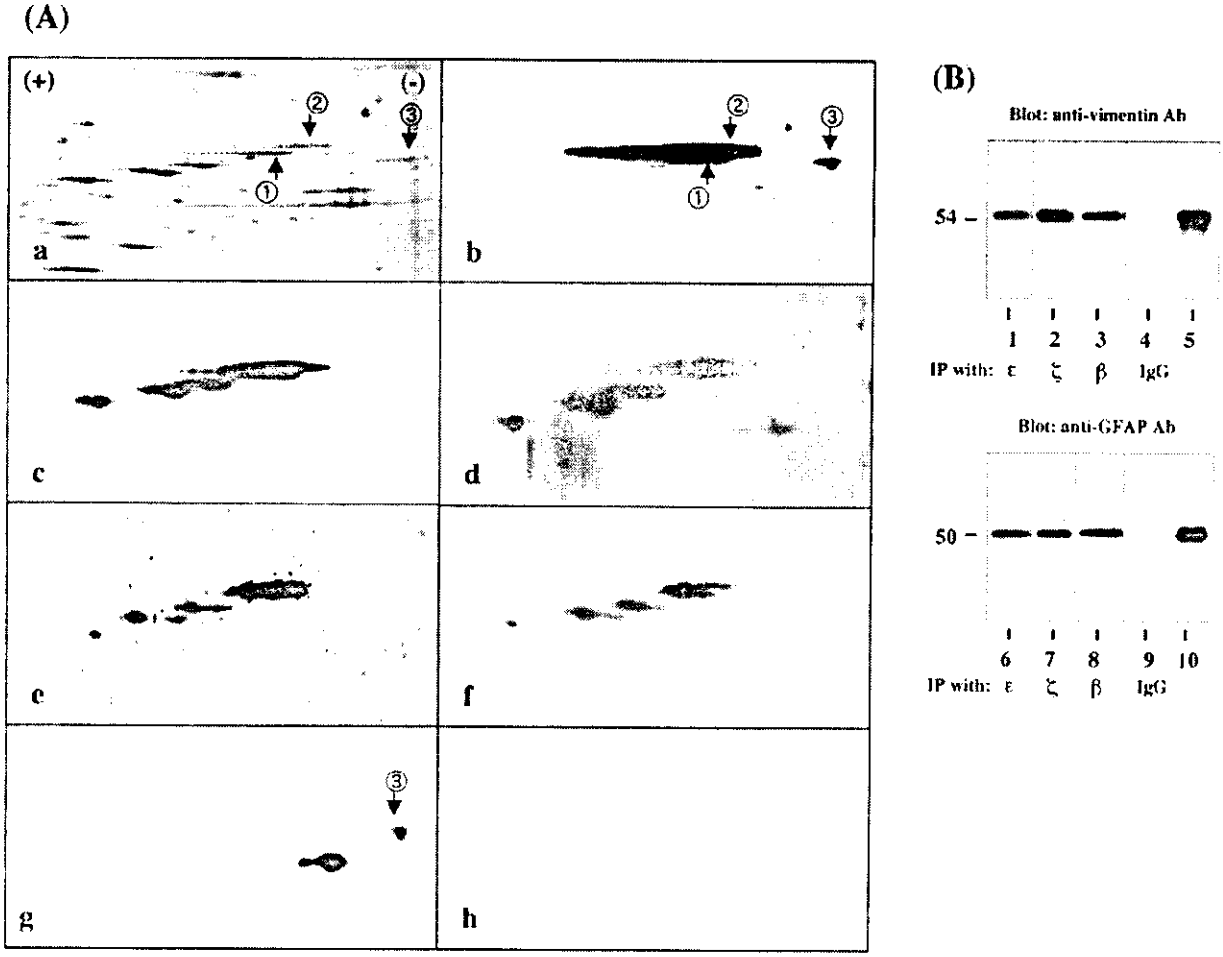

Figure 8. Two dimensional gel electrophoresis and immunoprecipitation analysis of 14-3-3 ε isoform binding proteins in cultured human astrocytes. **A:** Two dimensional gel analysis. Human astrocytes (AS BW) were incubated in 10% FBS containing culture medium. Twenty one μg of total protein extract was separated on a two dimensional PAGE gel, transblotted onto a polyvinylidene difluoride membrane, and processed for overlay analysis with recombinant human 14-3-3ε protein possessing the Xpress tag (rh14-3-3ε) followed by labeling with anti Xpress antibody. After the probe and antibody were stripped, the blot was repeatedly relabeled six times with the antibodies against GFAP, vimentin, and vimentin with specific phosphorylated serine epitopes, and with recombinant human interferon stimulated protein ISG15 having the Xpress tag (rhISG15). **a** to **g** represent silver staining (**a**), rh14-3-3ε labeling followed by staining with anti Xpress antibody (**b**), vimentin (**c**), vimentin with phosphorylated Ser 39 (**d**), vimentin with phosphorylated Ser 72 (**e**), vimentin with phosphorylated Ser 83 (**f**), GFAP (**g**), and rhISG15 labeling followed by staining with anti Xpress antibody (**h**). Two major spots labeled with rh14-3-3ε and anti vimentin antibody are named spot no. 1 and no. 2, while a spot labeled with rh14-3-3ε and anti GFAP antibody is designated spot no. 3. Spots no. 1 and no. 2 were excised from the gel and processed for mass spectrometry (MS) analysis. **B:** Immunoprecipitation analysis. Total protein extract of cultured human astrocytes was immunoprecipitated with ε isoform specific antibody (**lanes 1** and **6**), ζ isoform specific antibody (**lanes 2** and **7**), β isoform specific antibody (**lanes 3** and **8**), with the same amount of normal rabbit IgG (**lanes 4** and **9**), or untreated with any antibodies (**lanes 5** and **10**; 2 μg of total protein extract before processing for immunoprecipitation). Then, the immunoprecipitates were processed for Western blot analysis using anti vimentin (**top**) or anti GFAP antibody (**bottom**).

human brain homogenate, expressed substantial levels of β, γ, ε, ζ, η, and θ isoforms (Figure 1, a to h; lanes 1 to 4). In contrast, the σ isoform was undetectable in human neural cells but was identified in HeLa cells (Figure 1i, lanes 1 to 5).

To study the effects of culture conditions on 14-3-3 protein levels, human astrocytes were incubated for 7 days in 10% FBS-containing culture medium or in the serum-free culture medium, which led to nearly complete growth arrest. The expression levels of β, γ, ε, ζ, η, and θ isoforms were elevated in human astrocytes incubated in the serum-containing growth-promoting condition. The expression was enhanced 3.3-, 1.6-, 2.2-, 10.0-, 18.7-, or 4.6-fold, respectively, compared with the levels under the serum-free growth-arrested condition when standardized against the levels of HSP60, a housekeeping gene product on the identical blots (Figure 2, a to c, e to g; top and bottom panels, lanes 1 and 2). The serum-induced up-regulation of 14-3-3 isoforms was also observed in a different culture of human astrocytes (Figure 2d, top and bottom panels, lanes 1 and 2) and mouse astrocytes in culture (Figure 2h, top and bottom panels, lanes 1 and 2; and additional data shown in Supplementary Figure 2 on The American Journal of Pathology website at *http://www.amjpathol.org*). These results indicate that cultured human astrocytes constitutively express all iso-